ERRATA

NASA Technical Note D-5212

NOISE IN AXISYMMETRIC CONVERGENT ELECTRON BEAMS

by H. G. Kosmahl and L. U. Albers
May 1969

Page 11, equation (21): The first integral should read

$$\int_0^{\infty} dw\, e^{j\Theta_o\left[\vartheta_s(\xi)-\vartheta(\xi,w_i)\right]}\,\delta(w - w_i)$$

Page 11, equation (23): The integral should read

$$\int_0^{\infty} \left[wF_1(\xi,w_i,w) - \langle w\rangle F_1(\xi,w_i,w)\right]dw$$

Page 12, equation (25): The upper limit for the first integral should be ξ instead of ∞.

Page 16, line 6: "Equation (39)" should read "equation (35)."

Page 26, figure 7: The value for the anodal compression factor m given in the legend should be 2 instead of 3.

Page 27, figure 8: The value for the anodal compression factor m given in the legend should be 3 instead of 2.

Page 39, equation (B14a): The upper limit for the first integral should be ξ instead of ∞.

Page 49, equation (B45): The right side in the first line of the equation should read

$$\equiv \mathscr{L}^{-1}\left[F_{\nu}(p)\right] = \sum_{n=1}^{2} \operatorname{Res} F_{\nu}(p) e^{p_n \xi}$$

NASA TECHNICAL NOTE

NASA TN D-5212

NASA TN D-5212

NOISE IN AXISYMMETRIC CONVERGENT ELECTRON BEAMS

by H. G. Kosmahl and L. U. Albers

Lewis Research Center

Cleveland, Ohio

NATIONAL AERONAUTICS AND SPACE ADMINISTRATION • WASHINGTON, D. C. • MAY 1969

NASA TN D-5212

NOISE IN AXISYMMETRIC CONVERGENT ELECTRON BEAMS

By H. G. Kosmahl and L. U. Albers

Lewis Research Center
Cleveland, Ohio

NATIONAL AERONAUTICS AND SPACE ADMINISTRATION

For sale by the Clearinghouse for Federal Scientific and Technical Information
Springfield, Virginia 22151 – CFSTI price $3.00

ABSTRACT

The noise along axisymmetric convergent electron beams used in O-type high-power microwave tubes was investigated analytically as a function of several tube design parameters. The computations and investigations were carried out for magnetically fully confined flow, Brouillon flow, and electrostatically focused flow for power levels near 1 kW and perveances from 0.1×10^{-6} to 1.0×10^{-6}. The computed minimum noise figures ranged between 20 and 60 dB depending on voltage, perveance, area convergence, and gun design.

NOISE IN AXISYMMETRIC CONVERGENT ELECTRON BEAMS

by H. G. Kosmahl and L. U. Albers

Lewis Research Center

SUMMARY

The propagation of noise along axisymmetric convergent electron beams was calculated with the density function method by assuming one-dimensional motion with a variable cross section. The linearized Boltzmann equation was solved for the alternating-current distribution function by assuming half-Maxwellian direct-current distribution for two cases: a constant electron temperature and an electron temperature proportional to the beam-area-compression ratio.

The expressions for the AC noise current and electrokinetic voltage were derived from a Volterra-type integral equation and the noise power spectra and were then solved for a range of beam-gun parameters of interest in designs of medium-power and high-power tubes, that is, for power levels of 1 kilowatt or less, perveances between 0.1×10^{-6} to 1.0×10^{-6}, and total beam compressions up to 81.

The complex radiofrequency-noise convection current divided by the beam compression was shown to be invariant to area transformations, in that its application to variable-temperature cases leads to equations similar to those derived earlier for constant-cross-section, constant-temperature beams. At voltages higher than about 500 volts, the noise increases sharply with increasing voltage and approximately proportionately to beam perveances. For the same total beam compression, less final noise results if the initial preapertural compression is larger than the following compression. By judicious selection of gun-beam parameters, a significant reduction of noise by a few orders of magnitude can be achieved. The compiled noise figures ranged between 20 and 60 decibels, depending on compression ratio, perveance, and electron temperature.

INTRODUCTION

The nature and the propagation of thermal noise along electron beams that are used in O-type microwave amplifiers have been subject to numerous investigations over the past 15 years (refs. 1 to 7). Haus (refs. 1 and 2) has shown that the minimum noise

figure of any linear beam-type amplifier is determined by the knowledge of two basic noise parameters S and Π, which in turn can be determined from the noise power spectra of I_1 and U_1, the radiofrequency-noise convection current and the electrokinetic noise voltage, respectively. Analytical treatments of the noise convection current by the density function method, for which one-dimensional drifting beams, half-Maxwellian dc velocity distribution, and full uncorrelated shot noise at each velocity class (which lead to the problem of solving the well-known Volterra integral equation) are assumed, were given by Watkins (ref. 3) and Bloom and Vural (ref. 4), among others. For accelerated one-dimensional electron beams, Siegman, Watkins, and Hsieh, also using the density function method (refs. 5 and 6), carried out a numerical calculation of the noise fluctuations. To date, no investigations on convergent accelerated multivelocity beams are available. The investigation of Gandhi (ref. 8), which treats the transport of disturbances on electron beams under magnetic compression, assumes the constancy of S and Π and is, therefore, not valid for the propagation of noise in actual-multivelocity Maxwellian beams, along which both S and Π vary strongly with distance.

The advent of the space age, with its demands for ever higher frequencies combined with long life and the least possible power consumption, suggests the investigation of noise performance using convergent electron guns with axial symmetry (fig. 1). The rather respectable difficulties in solving a general multidimensional Boltzmann equation were avoided by using a "trick" frequently applied in fluid mechanics: to treat the problem as a one-dimensional motion but with a variable cross section. Between C and A (fig. 1) this approach amounts to solving the equation in spherical coordinates with the radius as the only variable and assuming independence of the polar angle and azimuth. The geometry of an idealized convergent gun is indeed that of a spherical cone (see fig. 1) symmetric about the O - O' axis, which goes through the center of the sphere, and with a

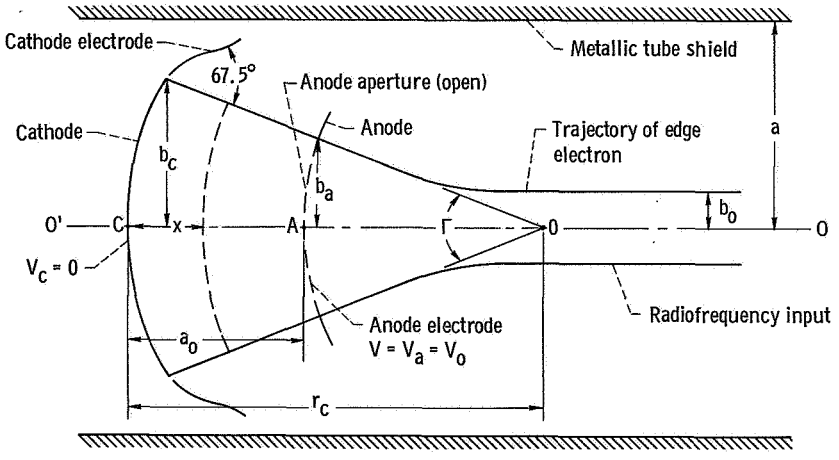

CD-10312-09

Figure 1. - Convergent electron gun.

solid angle Γ. The anode aperture A is a distance a_o away from the cathode C and, for a homocentric flow, all spherical shells $r_c - x$ = constant form equipotential lines.

Beyond the anode aperture, which constitutes a diverging lens, the trajectories are no longer homocentric but change into a drifting beam converging toward its minimum ultimate radius b_o. Therefore, an exponentially decreasing beam radius b was assumed for the region between the aperture and the axial distance at which b approaches b_o. Smooth transition between the two regions is assured by matching the radii and their slopes at the aperture.

In contrast to one-dimensional beams, along which the electron temperature T_e is or may be assumed constant, T_e increases along convergent beams. For constant current density across the beam, it may be shown with the help of statistical mechanics (refs. 9 and 10) that the transverse temperature increases proportionately to beam-area compression. Since - in O-type tubes - longitudinal beam fluctuations caused by the longitudinal electron temperature are amplified, the question arises as to the relation between the transverse and longitudinal temperatures. For the case of confined flow guns, with a strong magnetic flux cutting through the cathode, the transverse electron fluctuations are converted into longitudinal noise as a result of the adiabatic conservation of the electron dipole moment. Thus, in this case, both the transverse and the longitudinal temperatures are proportional to the beam-area compression.

For Brouillon-type guns, or guns fully shielded from magnetic fields, little or no conversion of transverse into longitudinal fluctuations (in absence of collisions) will occur until the electrons enter the converging magnetic field region beyond the aperture. At this position, however, the stream has reached its final dc velocity and the velocity spread is small. On the other hand, all "practical" Brouillon-type guns have a small amount of flux cutting through the cathode so that a partial conversion of transverse into longitudinal noise is probable, too.

The last case to be considered herein is the purely electrostatically focused guns characterized by a complete absence of any magnetic focusing fields. Again, in absence of true coulomb collisions, two different temperatures, T_l and T_t, may exist independently, and an increase of T_t with compression will probably not lead to an equivalent buildup of T_l. Thus, $T_l \approx T_c$ = constant seems more appropriate, and a converging beam with an approximately constant longitudinal temperature is dealt with. Both cases, that of T_l = constant and T_l proportional to area compression ratio A_R, are treated subsequently by machine calculations and approximate closed-form solutions to permit extrapolations between these two temperature limits.

The integration of the ac density function over the velocity spread leads to a Volterra-type integral equation for the noise convection current. The integration of this Volterra equation with a beam having a variable density and a variable cross section requires knowledge of the reduced plasma frequency and, thus, the plasma frequency reduction factor R. The value of R has been computed for constant-velocity, constant-diameter

beams (ref. 11). For variable-velocity beams with changing diameters, exact expressions for R are not available, and no attempt was made to obtain an exact solution in the present study. However, R is not much different from 1 in the cathode-anode region, and the introduction of approximate values for R does not change the final result by more than 5 to 10 percent compared with the case R = 1. This problem is treated in appendix A.

In order to obtain an insight into the physics of the noise phenomena in convergent accelerated beams, in addition to accurate computation results, the nonlinear transit time function in the Volterra integral equation was expanded in a Taylor series around a suitable center and linearized. The resulting integral equation was then solved by the Laplace transformation method, thus permitting a comparison with cases previously treated for constant-velocity, constant-temperature, and constant-diameter beams (appendix B).

The computational method chosen and the problems and difficulties in numerically solving the Volterra integral equation were treated separately in appendix C. An excellent check for the accuracy of the computations is the amount by which the total noise (e.g., radiofrequency) power $S + \Pi$ deviates from 1 for constant-temperature streams.

The power series for the Langmuir-Blodgett potential is derived in appendix D.

The significance of the investigation lies in the fact that it permits designing medium- and high-power O-type tubes that will have more favorable noise performance while utilizing convergent guns. The results of this study become particularly important for all cases with relatively low output powers (1 kW or less), relatively large bandwidths (FM), and relatively large beam compressions (high microwave frequencies), since they permit signal-to-noise-ratio designs of 50 decibels or more without the need of unnecessarily increasing the output power, even in multichannel, wide-bandwidth systems. In view of the fact that our ability to generate microwave power decreases with frequency as $f^{-5/2}$, the preceding arguments are self-explanatory.

The International System of Units is used throughout this report. The reader is referred to appendix E for definitions of the most important quantities.

ANALYSIS

The analysis of the noise propagation problem along convergent beams with the density function method is in the next sections and is based on the following assumptions:

(1) The Boltzmann equation may be linearized and is collisionless.

(2) The motion is considered one dimensional but has a variable cross section.

(3) The longitudinal electron temperature T_l is either constant or proportional to the area compression ratio A_R.

(4) The direct-current potential distribution is that given by the Langmuir-Blodgett series.

(5) Fully uncorrelated shot noise at each velocity class is injected into the direct-current stream at a 90° angle to the cathode.

(6) The total alternating current in the gun is zero.

(7) The velocity distribution is half Maxwellian because of an almost complete absence of collisions between electrons for the range of densities and temperatures applicable to microwave tubes.

Variable-Temperature Case

The analysis begins with the more general case of variable temperature. The collisionless Boltzmann equation, written for one dimension, is (ref. 6)

$$\frac{df(x,u,t)}{dt} = \frac{\partial f}{\partial t} + u\frac{\partial f}{\partial x} + \frac{du}{dt}\frac{\partial f}{\partial u} = 0 \tag{1}$$

where x designates the distance along the electron trajectory, $f(x,u,t) = f_o(x,u) + f_1(x,u)e^{j\omega t}$ are the direct-current and alternating-current distribution functions, and the time dependence varies as $e^{j\omega t}$. In the present case, since $f_o >> f_1$, equation (1) may be linearized by neglecting products of two alternating-current quantities. Let $E_o(x)$ and $E_1(x)$ be the direct-current and alternating-current fields, respectively. The alternating part of equation (1) will then assume the form

$$j\omega f_1 + u\frac{\partial f_1}{\partial x} + \eta E_1\frac{\partial f_o}{\partial u} + \eta E_o\frac{\partial f_1}{\partial u} = 0 \tag{2}$$

with $\eta = e/M_e$.

Conventional Noise Relations

The following conventional notations in noise terminology are used:

$$u_s^2(a_o) = 2\eta V_a; \quad u^2(x) = u_s^2(x) + \frac{w}{\alpha_T}; \quad 2\eta V_a = \frac{1}{2\alpha_T\sigma_T} = \frac{1}{2\alpha_o\sigma_o}$$

$$w = \alpha_T\left(u^2 - u_s^2\right) = \alpha_T\left[u^2 - 2\eta V_o(x)\right]; \quad u = u_s\left[1 + 2\sigma_T\frac{V_a}{V_o(x)}w\right]^{1/2}$$

$$\alpha_T = \frac{M_e}{2kT(x)} = \alpha_o\left(1 - \frac{x}{r_c}\right)^2 \qquad \text{for } 0 \le x \le a_o \text{ or } \alpha_T = \frac{\alpha_o}{A_R(x)}$$

$$\sigma_T = \frac{kT(x)}{2eV_a} = \frac{\sigma_o}{\left(1 - \frac{x}{r_c}\right)^2} \qquad \text{for } 0 < x \le a_o \text{ or } \sigma_T = \sigma_o \cdot A_R(x)$$

$$\alpha_o = \frac{M_e}{2kT_c}; \quad \sigma_o = \frac{kT_c}{2eV_a}; \quad \lambda_a = \frac{\omega_{pas}}{\omega}$$

$$\omega_q = R \cdot \omega_p; \quad \omega_{qs}^2(x) = \frac{\eta i_o(x)}{\epsilon_o u_s(a_o)} \cdot R^2(x); \quad \omega_{pas}^2 = \frac{\eta i_o(a_o)}{\epsilon_o u_s(a_o)}$$

$$E(x) = \frac{\partial V(x)}{\partial x}; \quad f_o(x_1 w) = 2\alpha_T i_o(x) \cdot g(w) = 2\alpha_T i_o(x) S(w) e^{-w}$$

$$\frac{\partial f_o}{\partial w} = 2\alpha_T i_o(x)\left[\delta(w) - S(w)\, e^{-w}\right]$$

Cathode-Aperture Region

Next, the distribution function $f(x, u)$ is transformed into $F[x, w(x, u)]$ using the method of reference 5 for the region $0 \le x \le a_o$

$$\frac{\partial f_1}{\partial x} = \frac{\partial F_1}{\partial x} + \frac{\partial F_1}{\partial w}\frac{\partial w}{\partial x} = \frac{\partial F_1}{\partial x} - 2\alpha_T \eta E_o \frac{\partial F_1}{\partial w} - \frac{2\alpha_o}{r_c}\left(1 - \frac{x}{r_c}\right)\frac{\partial F_1}{\partial w}\left[u^2 - 2\eta V_o(x)\right] \qquad (3a)$$

and

$$\frac{\partial f_o}{\partial u} = \frac{\partial F_o}{\partial w}\frac{\partial w}{\partial x} = 2\alpha_T u \frac{\partial F_o}{\partial w} = 2\alpha_T 2\alpha_T i_o(x) \frac{\partial g}{\partial w} u \qquad (3b)$$

to obtain

$$j\omega F_1 + u\left[\frac{\partial F_1}{\partial x} + 4\alpha_o^2\eta\left(1 - \frac{x}{r_c}\right)^4 i_o(x)E_1(x)\frac{\partial g}{\partial w} - \frac{\partial F_1}{\partial w}\frac{2}{r_c}\frac{w}{1 - \frac{x}{r_c}}\right] = 0 \tag{4}$$

In a radiofrequency open circuit (total current equal to zero), the relation between the convection current density $i_1(x)$ and the radiofrequency field E_1 is from Maxwell's equations:

$$R^2(x)i_1(x) + j\omega\epsilon_o E_1(x) = 0 \tag{5}$$

An approximate expression for $R(x)$, the plasma-frequency reduction factor, is derived in appendix A. From the basic definition of F_1, i_1 is obtained by integrating over all velocity classes:

$$i_1(x) = \frac{1}{2\alpha_T}\int_0^\infty F_1(x, w)\,dw \tag{6}$$

Equation (4) is a linear, partial differential equation for $F_1(x, w)$. Note that ordinary differential equations are obtained for $F_1(x, w)$ (refs. 3 to 6) for constant-diameter, constant-temperature streams. Equation (4) is solved by writing it in the form

$$r_c\left(1 - \frac{x}{r_o}\right)\frac{\partial F_1}{\partial x} - 2w\frac{\partial F_1}{\partial w} = -r_c\frac{\left(1 - \frac{x}{r_c}\right)}{u(x)}\left[j\omega F_1 + 4\alpha_o^2\eta\left(1 - \frac{x}{r_c}\right)^4 i_o(x)\frac{\partial g}{\partial w}E_1(x)u(x)\right] \tag{7}$$

For compactness,

$$4\alpha_o^2\eta\left(1 - \frac{x}{r_e}\right)^4 i_o(x)\frac{\partial g}{\partial w}E_1(x) = H(x, w) \tag{8}$$

The equations of characteristics, derivable from equation (7), are

$$\frac{dx}{r_c\left(1 - \frac{x}{r_c}\right)} = -\frac{dw}{2w} = -\frac{dF_1(x, w)}{\left[\frac{j\omega F_1(x, w)}{u(x, w)} + H(x, w)\right]r_c\left(1 - \frac{x}{r_c}\right)} \tag{9}$$

Solving the first of the equations yields

$$w = C_1 \left(1 - \frac{x}{r_c}\right)^2 \tag{10}$$

After substituting w from equation (10) into the first and third equality terms of equation (9), an ordinary differential equation for F_1 is obtained:

$$\frac{dF_1}{dx} + j \frac{\omega}{u(x)} F_1 + H(x, c_1) = 0, \tag{11}$$

since, using equation (10) yields

$$u(x, w) = (2\eta V_a)^{1/2} \left[\frac{V_o(x)}{V_a} + 2\sigma_T w\right]^{1/2} = (2\eta V_a)^{1/2} \left[\frac{V_o(x)}{V_a} + 2\sigma_o c_1\right]^{1/2} \tag{12}$$

New dimensionless variables are introduced:

$$\xi = \frac{x}{a_o} \qquad \frac{\partial}{\partial x} = \frac{1}{a_o} \frac{\partial}{\partial \xi}; \qquad \Theta_o = \frac{\omega \cdot a_o}{u_s(a_o)} = \frac{\omega \cdot a_o}{(2\eta V_a)^{1/2}} \tag{13}$$

and the following transit time functions are defined:

$$\vartheta_s(\xi) = \int_0^{\xi} \frac{d\xi'}{\sqrt{\frac{V(\xi')}{V_a}}} \tag{14a}$$

$$\vartheta(\xi, c) = \int_0^{\xi} \frac{d\xi'}{\left[\frac{V(\xi')}{V_a} + 2\sigma_o c_1\right]^{1/2}} \tag{14b}$$

$$\vartheta(\xi, w) = \int_0^{\xi} \frac{d\xi'}{\left[\frac{V(\xi')}{V_a} + 2\,\frac{\sigma_o w}{\left(1 - \frac{a_o}{r_c}\,\xi'\right)^2}\right]^{1/2}} \tag{14c}$$

The general solution of equation (11) may now be written with the help of equations (12) to (14) in the form

$$F_1(\xi, C) = c_2 e^{-j\Theta_o \vartheta(\xi, c_1)} - a_o \int_0^{\xi} H(\xi', c_1) e^{-j\Theta_o \left[\vartheta(\xi, c_1) - \vartheta(\xi', c_1)\right]} d\xi' \tag{15}$$

If c_1 is replaced by its value, $c_1 = w/\left[1 - (x/r_c)\right]^2$ from equation (10), and if equation (15) is solved for the new integration constant c_2, the following equation is obtained:

$$c_2 = F(\xi, w) e^{+j\Theta_o \vartheta(\xi, w)} + a_o e^{+j\Theta_o \vartheta(\xi, w)} \int_0^{\xi} H(\xi', c) e^{-j\Theta_o \left[\vartheta(\xi, w) - \vartheta(\xi, w)\right]} d\xi'$$

$$= G(c_1) \equiv G\left[\frac{w}{\left(1 - \frac{x}{r_c}\right)^2}\right] = G\left[\frac{w}{\left(1 - \frac{a_o \xi}{r_c}\right)^2}\right] \tag{16}$$

where G is an arbitrary function of $c_1(x, w) = w/\left[1 - (x/r_c)\right]^2$. In accordance with the seven analytical assumptions, the initial value condition for the noise injection at the cathode $x = 0$ (potential minimum) is given by fully uncorrelated shot current in each velocity class w_i independent of other fluctuations w. Thus, because of equations (6) and (16),

$$F_1(0, w_i) \equiv G(w_i) = 2\alpha_o \cdot i_1(0, w_i)\delta(w - w_i) = 2\alpha_o \delta(w - w_i) \tag{17}$$

where $i_1(0, w_i)$ has been normalized to 1. Equation (15) is now put into the form

$$F(\xi, w_i, w) = F_1(0, w_i)e^{-j\Theta_o \vartheta(\xi, w_i)} + \frac{4\alpha_o^2 \lambda_a^2}{j} \frac{\partial g}{\partial w} \left(1 - \frac{a_o}{r_c}\right)^2 \theta_o \cdot 2\eta V_a$$

$$\times \int_0^{\xi} R_1^2(\xi') \left(1 - \frac{a_o}{r_c} \xi'\right)^2 i_1(\xi') e^{-j\Theta_o \left[\vartheta(\xi, w) - \vartheta(\xi', w)\right]} d\xi' \qquad (18)$$

In writing equation (18), the direct-current continuity equation for $i_o(x) = i_o(a)A(a_o)/A(x)$ and equations (5) and (8) were used. Since $\alpha_T \cdot \sigma_T = \alpha_o \sigma_o = 1/4\eta V_a$, equation (18) is put into its final form:

$$F_1(\xi, w_i, w) = F_1(0, w_i)e^{-j\Theta_o \vartheta(\xi, w_i)} + \frac{2\alpha_o}{j\sigma_o} \lambda_a^2 \frac{\partial g}{\partial w} \left(1 - \frac{a_o}{r_c}\right)^2 \Theta_o$$

$$\times \int_0^{\xi} R_1^2(\xi') \left(1 - \frac{a_o}{r_c} \xi'\right)^2 i_1(\xi') e^{-j\Theta_o \left[\vartheta(\xi, w) - \vartheta(\xi', w)\right]} d\xi' \qquad (19)$$

The defining equation is

$$I_1(\xi, w_i) = \frac{1}{2\alpha_T} \int_0^{\infty} F_1(\xi, w_i, w) e^{j\Theta_o \vartheta_s(\xi)} dw \equiv i_1(\xi, w_i) e^{j\Theta_o \vartheta_s(\xi)} \qquad (20)$$

If equation (20) is applied to equation (19), the following expression for $I_1(\xi, w_i)$ is obtained:

$$I_1(\xi, w_i) = \frac{2\alpha_o}{2\alpha_T} \int_0^\infty e^{j\Theta_o\left[\vartheta_s(\xi) - \vartheta(\xi, w_i)\right]} \, (w - w_i) + \frac{\lambda_a^2}{j\sigma_o} \frac{\left(1 - \frac{a_o}{r_c}\right)^2 \Theta_o}{\left(1 - \frac{a_o}{r_c}\,\xi\right)^2}$$

$$\times \int_0^\xi \left(1 - \frac{a_o}{r_c}\,\xi'\right)^2 R^2(\xi') i_1(\xi') \, d\xi' \left\{ \int_0^\infty \delta(w) e^{-w_e j\Theta_o\left[\vartheta_s(\xi) - \vartheta(\xi, w) + \vartheta(\xi', w)\right]} \, dw \right.$$

$$\left. - \int_0^\infty S(w) e^{-w_e j\Theta_o\left[\vartheta_s(\xi) - \vartheta(\xi, w) + \vartheta(\xi', w)\right]} \, dw \right\} \tag{21}$$

After the singularities are removed by applying standard relations concerning S and δ, the final expression for $I_1(\xi, w_i)$ can be reduced to

$$I_1(\xi, w_i) = \frac{e^{j\Theta_o\left[\vartheta_s(\xi) - \vartheta(\xi, w_i)\right]}}{\left(1 - \frac{a_o}{r_c}\,\xi\right)^2} + \frac{\lambda_a^2}{j\sigma_o} \frac{\left(1 - \frac{a_o}{r_c}\right)^2 \Theta_o}{\left(1 - \frac{a_o}{r_c}\,\xi\right)^2} \int_0^\xi R^2(\xi') \left(1 - \frac{a_o}{r_c}\,\xi'\right)^2 I_1(\xi', w_i)$$

$$\times \left(1 - \int_0^\infty e^{-w_e j\Theta_o\left\{\vartheta_s(\xi) - \vartheta_s(\xi') - \left[\vartheta(\xi, w) - \vartheta(\xi', w)\right]\right\}} \, d\xi' \, dw \right) \tag{22}$$

Equation (22) is the well-known Volterra-type integral equation of the noise current I_1 derived herein for the general case of a variable-cross-section, variable temperature electron stream with azimuthal symmetry. In addition to I_1, the second quantity that is needed for the calculation of the noise performance is the electrokinetic voltage $U(\xi, w_i)$, which is defined in references 1 and 2 as

$$U(\xi, w_i) = \frac{1}{2\alpha_T} e^{j\Theta_o \vartheta_s(\xi)} \int_0^\infty w F_1(\xi, w_i, w) - \langle w \rangle F_1(\xi, w_i, w) \, dw \tag{23}$$

Since, for half-Maxwellian direct-current distribution,

$$\langle w \rangle = \int_0^\infty w g(w)\, dw = 1 \tag{24}$$

the following equation is obtained from equations (19), (23), and (24):

$$U(\xi, w_i) = -I_1(\xi, w_i) + \frac{w_i}{\left(1 - \frac{a_o}{r_c}\xi\right)^2} e^{j\Theta_o\left[\vartheta_s(\xi) - \vartheta(\xi, w_i)\right]}$$

$$- \frac{\lambda_a^2}{j\sigma_o} \frac{\left(1 - \frac{a_o}{r_c}\right)^2}{\left(1 - \frac{a_o}{r_c}\xi\right)^2} \Theta_o \int_0^\infty R^2(\xi') \left(1 - \frac{a_o}{r_c}\xi'\right)^2 I_1(\xi', w_i)$$

$$\times \int_0^\infty e^{-j\Theta_o\left\{\vartheta_s(\xi) - \vartheta_s(\xi') - \left[\vartheta(\xi, w) - \vartheta(\xi', w)\right]\right\}} w e^{-w}\, dw\, d\xi' \tag{25}$$

From equations (14a) and (14c), the transit time functions $\vartheta_s(\xi)$ and $\vartheta(\xi, w)$ contain the ratios $V(\xi)/V(1) = V(x)/V_a$; that is, the direct-current potential distribution in a spherical electron gun. This distribution has been computed by Langmuir and Blodgett (ref. 11) for zero velocity at the cathode. Although the velocity spread due to the Maxwell-Boltzmann distribution does change the potential profile in the vicinity of the emitter compared with the case of no spread, the effect is negligibly small for an anode potential greater than 10 volts. On the other hand, note that full account is taken of the velocity spread in the beam itself by the direct-current distribution function $f_o = 2\alpha_T i_o(x) S(w) e^{-w}$. Refer now to figure 1 and reference 13, where $r_c > r_a$, and $x = r$:

$$V(x) = V(r) = V(a_o) \frac{\alpha^{4/3}\left(\frac{r}{r_c}\right)}{\alpha^{4/3}\left(\frac{r_a}{r_c}\right)} \tag{26a}$$

$$V(\xi) = V_{a_o} \frac{\alpha^{4/3}\left(\frac{r}{r_c}\right)}{\alpha^{4/3}\left(\frac{r_a}{r_c}\right)} \tag{26b}$$

In appendix D, $\alpha(r/r_c) = \alpha\left[\xi(a_o/r_c)\right]$ is shown to be represented by the power series, equation (D3):

$$\alpha\left(\xi \frac{a_o}{r_c}\right) = \alpha(y\xi) = -y\xi\left(1 + \frac{4}{5}y\xi + \frac{17}{24}y^2\xi^2 + 0.652y^3\xi^3 + \ldots\right) \tag{D3}$$

The values for α may be obtained from table II in reference 13.

Anode Minimum-Beam-Diameter Region

The preceding analysis was applied to the cathode-anode region, $0 \leq \xi \leq 1$. Because the radiofrequency input of the tube is located in the vicinity of the minimum beam diameter at approximately $\xi = 2$, both $I_1(2)$ and $U_1(2)$ must be known to determine the noise performance of the tube. Beyond the anode aperture, which constitutes a diverging lens, the trajectories no longer remain homocentric but change into a drifting beam that gradually converges toward its ultimate minimum radius b_o at approximately $\xi = 2$. Therefore, the following approximation for the beam profile is made in the region $1 < \xi \leq 2$

$$b(\xi) = b_o e^{-\kappa(\xi) \cdot \xi} \tag{27}$$

where $\kappa(\xi)$ is an appropriate polynomial in ξ, such that $b(\xi)$ decreases monotonically to the asymptotic value of b_o at $\xi = 2$. Moreover, the initial value conditions are

$$b_a = b(\xi)_{\xi=1} = mb_o \tag{28a}$$

$$b'(\xi)_{\xi=1} = -\tan\frac{\Gamma}{2} \approx -\frac{mb_o}{r_o - a_o} \tag{28b}$$

$$b(\xi)_{\xi=2} = b_o \tag{28c}$$

$$b'(\xi)_{\xi=2} = 0 \tag{28d}$$

In equation (28b), $\tan \Gamma/2$ has been replaced by $\sin \Gamma/2$. This approximation is valid for small angles, $\Gamma < 10^o$. The conditions of equations (28) provide a smooth transition for the beam size and its slope from region $\xi \leq 1$ into $\xi \geq 1$. They are easily derived from figure 1. The condition of equation (28a), fixes the ratio $m > 1$ of the beam radius at the aperture $\xi = 1$ and b_o at $\xi \approx 2$. From equations (28),

$$b_o e^{-\kappa(1)} = m b_o ; - \left[\kappa(1) + \kappa(1)\right] b_o e^{-\kappa(1)} = - \frac{m b_o}{r_c - a_o} \tag{29a}$$

$$b_o e^{-2\kappa(2)} = b_o ; - \left[2\kappa(2) + \kappa(2)\right] e^{-2\kappa(2)} = 0 \tag{29b}$$

The compression ratio in the beam cross section A_R, referred to the beam cross section at the cathode, is

$$A_R(\xi) = \frac{b_c^2}{b^2(\xi)} = \frac{1}{\left(1 - \frac{a_o}{r_c}\,\xi\right)^2} \qquad \text{for } 0 \leq \xi \leq 1 \tag{30a}$$

$$A_R(\xi) = \frac{b_c^2}{b^2(\xi)} = \frac{m^2}{\left(1 - \frac{a_o}{r_c}\right)^2} e^{2\kappa(\xi) \cdot \xi} \qquad \text{for } 1 \leq \xi \leq 2 \tag{30b}$$

The transit time functions $\vartheta_s(\xi)$ and $\vartheta(\xi, w)$ from equation (14) simplify now with $V(\xi') = V(1) = V_a$ for $\xi' \geq 1$:

$$\vartheta_s(\xi) = \int_0^{\xi} \frac{d\xi'}{\left[\frac{V(\xi')}{V(1)}\right]^{1/2}} \tag{31a}$$

$$\vartheta(\xi, w) = \int_0^{\xi} \frac{d\xi'}{\left[\frac{V(\xi')}{V(1)} + 2\sigma_o w \cdot A_R(\xi')\right]^{1/2}} \tag{31b}$$

Note that, because of the transformation of $f(x, w)$ into $F(x, w(x, u))$, the direct-current acceleration due to E_o (which is zero for $\xi \geq 1$) drops out from equation (4). Therefore, equations (4), (22), and (25) may be used for calculating F_1, I_1, and U_1 in the region $\xi \geq 1$, provided that the compression ratios $A_R(\xi)$ (eqs. (30)) and the transit time functions occurring in them are replaced by equations (30) and (31), respectively. Thus, the following equation is obtained in general for $0 < \xi \leq 2$:

$$I_1(\xi, w_i) = e^{j\Theta_o\left[\vartheta_s(\xi) - \vartheta(\xi, w_i)\right]} A_R(\xi) + \frac{\lambda_a^2}{j\sigma_o}\Theta_o \left(1 - \frac{a_o}{r_e}\right)^2 A_R(\xi) \int_{\xi'=0}^{\xi} R^2(\xi') \frac{I_1(\xi', w_i)}{A_R(\xi')}$$

$$\left\{1 - \int_0^{\infty} e^{-w + j\Theta_o\left[\vartheta_s(\xi) - \vartheta_s(\xi') - \vartheta(\xi, w) + \vartheta(\xi', w)\right]} dw\, d\xi'\right\} \tag{32}$$

$$U_1(\xi, w_i) = -I_1(\xi, w_i) + w_i A_R(\xi) \cdot e^{j\Theta_o\left[\vartheta_s(\xi) - \vartheta(\xi, w_i)\right]}$$

$$- \frac{\lambda_a^2}{j\sigma_o}\left(1 - \frac{a_o}{r_c}\right)^2 \Theta_o\, A_R(\xi) \left\{\int_0^{\xi} R^2(\xi') \frac{I_1(\xi, w_i)}{A_R(\xi')}\right.$$

$$\left. \times \int_0^{\infty} e^{-w + j\Theta_o\left[\vartheta_s(\xi) - \vartheta_s(\xi') - \vartheta(\xi, w) + \vartheta(\xi', w)\right]} dw\, d\xi'\right\} \tag{33}$$

Note that, because of the character of the Volterra equation, its integration must proceed over the entire range $0 \leq \xi' \leq \xi$ by applying the expressions for I and U within their respective range of validity. Equation (32) permits an important transformation: $I_1(\xi, w_i)$ is divided by $A_R(\xi)$, the beam compression, and a new function $J_1(\xi, w_i)$ is defined as

$$J_1(\xi, w_i) \equiv \frac{I_1(\xi, w_i)}{A_R(\xi)} \tag{34}$$

Equation (32) can then be put into the form

$$J_1(\xi, w_i) = e^{j\Theta_o\left[\vartheta_s(\xi)-\vartheta(\xi, w_i)\right]} + \frac{\lambda_a^2}{j\sigma_o}\left(1 - \frac{a_o}{r_c}\right)^2 \Theta_o \int_{\xi'=0}^{\xi} R^2(\xi') J_1(\xi', w_i)$$

$$\times \left\{1 - \int_0^{\infty} e^{-w+j\Theta_o\left[\vartheta_s(\xi)-\vartheta_s(\xi')-\vartheta(\xi, w)+\vartheta(\xi', w)\right]} d\xi'\, dw\right\} \tag{35}$$

If $\lambda_a^2\left[1 - (a_o/r_c)^2\right]\Theta_o \cdot R^2(\xi)$ is considered as a kind of a modified plasma frequency, equation (39) for $J_1(\xi, w_i)$ is similar to that obtained earlier by Bloom and Vural (ref. 4) for the simpler case of a constant-velocity, constant-temperature, and constant-cross-section stream. Since the stream is still Maxwellian, all conclusions valid for I_1 apply as well to J_1. Especially, $S + \Pi = 1$ for constant temperature beams with I_1 must also hold for functions derived from J_1. Moreover, since I_1 (in ref. 4) may be considered as the complex noise current divided by the unity compression ratio, J_1 is, in general, an invariant to compressions, but I_1 is not, at least as long as the stream is one dimensional but with a variable cross section, Maxwellian and axisymmetric

Constant Longitudinal Temperature

The case of constant longitudinal temperature T_L can be easily obtained from the equations developed in this section. For α_o and σ_o, remaining constant, equation (4) simplifies to

$$j\omega F_1 + u(x)\left[\frac{\partial F_1}{\partial x} + 4\alpha_o^2 \eta i_o(x) E_1(x) \frac{\partial g}{\partial w}\right] = 0 \tag{36}$$

which is now an ordinary differential equation for $F_1(x, u)$. The transit time function $\vartheta_s(\xi)$ (eq. (14a)) remains unchanged and, since $V(\xi') \equiv V(1)$ for $\xi' \geq 1$, equation (14c) becomes

$$\vartheta_o(\xi, w) = \int_{\xi'=0}^{\xi} \frac{d\xi'}{\left(\frac{V(\xi')}{V_a} + 2\sigma_o w\right)^{1/2}} \tag{37}$$

After integrating $F_1(x, w)$, the following equations for the noise convection current $I_{1,o}(\xi, w_i)$ and the electrokinetic voltage $U_{1,o}(\xi, w_i)$ along a beam with a constant longitudinal temperature and a variable cross section are obtained:

$$I_{1,o}(\xi, w_o) = e^{j\Theta_o\left[\vartheta_s(\xi)-\vartheta_s(\xi, w_i)\right]} + \frac{\lambda_a^2}{j\sigma_o}\left(1 - \frac{a_o}{r_c}\right)^2 \Theta_o \int_{\xi'=0}^{\xi=\xi} R^2(\xi') I_{1,o}(\xi', w_i) \cdot A_R(\xi')$$

$$\times \left\{1 - \int_0^{\infty} e^{-w+j\Theta_o\left[\vartheta_s(\xi)-\vartheta_s(\xi')-\vartheta_o(\xi, w)+\vartheta_o(\xi', w)\right]} dw\, d\xi'\right\} \tag{38}$$

$$U_{1,o}(\xi, w_i) = -I_{1,o}(\xi, w_i) + w_i e^{j\Theta_o\left[\vartheta_s(\xi)-\vartheta_o(\xi, w_i)\right]} - \frac{\lambda_a^2}{j\sigma_o}\left(1 - \frac{a_o}{r_c}\right)^2 \Theta_o \int_{\xi'=0}^{\xi} R^2(\xi')$$

$$\times I_{1,o}(\xi', w_o) \cdot A_R(\xi') \int_0^{\infty} w e^{-w} e^{j\Theta_o\left[\vartheta_s(\xi)-\vartheta_s(\xi')-\vartheta_o(\xi, w)+\vartheta_o(\xi', w)\right]} dw\, d\xi' \tag{39}$$

Noise Power Spectra

At this point in the analysis, the noise power spectra can be calculated by averaging $|U|^2$, $|I|^2$, and $I \cdot U^*$ over the half-Maxwellian distribution (ref. 1). From reference 1 are obtained

$$\psi(\xi) = \langle |I(\xi, w_i)|^2 \rangle \int_0^{\infty} |I(\xi, w_i)|^2 e^{-w_i} dw_i \tag{40}$$

$$\Phi(\xi) = \langle |U(\xi, w_i)|^2 \rangle \equiv \int_0^{\infty} |U(\xi, w_i)|^2 e^{-w_i} dw_i \tag{41}$$

$$\Pi(\xi) + j\Lambda(\xi) = \langle I(\xi, w_i) \cdot U^*(\xi, w_i) \rangle \equiv \int_0^\infty I(\xi, w_i) U^*(\xi, w_i) e^{-w_i} \, dw_i \tag{42}$$

$$S(\xi) = \left[\psi(\xi) \cdot \Phi(\xi) - \Lambda^2(\xi)\right]^{1/2} \tag{43}$$

In equations (40) to (43), either I_1 and U_1 or $I_{1,o}$ and $U_{1,o}$ should be used. Haus (refs. 1 and 2) has shown that the minimum possible noise figure of any linear electron beam amplifier is given by the expression

$$F_{min}(\xi) = 1 + \left[S(\xi) - \Pi(\xi)\right] \frac{T_c}{T_o} \tag{44a}$$

Of particular importance to the present analysis is the value of $F_{min}(\xi)_{\xi=2}$, which, after it is multiplyed by kT_o times the bandwidth, represents the least possible noise power at the signal input of the amplifier. The cathode temperature T_c is equal to the physical temperature of the cathode surface. Note that, in the present definition, both S and Π are normalized dimensionless noise spectral functions.

Equation (44a) is valid strictly for lossless circuits. For practical interaction circuits, $(S - \Pi)$ in equation (44a) should be multiplied by the factor $\left[1 + (d/x_1)\right]$, where d and x_1 are the loss parameter and growing wave parameter, respectively. For narrow-bandwidth (e.g., < 5 percent) high-impedance-interaction circuits, such as cavities, this factor is very close to 1. For wide-band tubes (e.g., helical circuits), the factor may be as high as 1.2 to 1.5 in the frequency range of interest ($\lesssim$ 12 GHz).

For $F_{min} >> 1$, as is the case in power tubes, a very accurate approximation is obtained by neglecting 1 in equation (44a). Thus,

$$F_{min}(\xi) \simeq \left[S(\xi) - \Pi(\xi)\right] \frac{T_c}{293} \tag{44b}$$

RESULTS AND DISCUSSION

Choice of Parameters for Medium- and High-Power Tubes

Before the computational and analytical results are reviewed, the meaning and the range of beam-gun design parameters are discussed. It should be borne in mind that the selection of these parameters is dictated by power tube requirements, such as efficiency,

gain, and beam transmission, and not by minimum noise requirements. Therefore, the results of this study, if carried out over a suitable range of typical numbers, show representative noise levels associated with power tube designs. The beam-gun parameters used in this study are Θ_o, a_o/r_c, λ_a, σ, b_o, and m.

By definition, $\Theta_o = \omega \cdot a_o/(2\eta V_o)^{1/2} = (\omega/u_o)a_o$ is the transit time in radians (in the absence of space charge) of an electron having the full anode velocity $u_o = 2\eta V_o^{1/2}$ all the way between cathode and anode. The actual transit time is, of course, larger than Θ_o and is given by $\vartheta(\xi, w_i) \cdot \Theta_o$. However, Θ_o is proportional to the distance cathode-anode a_o and is therefore an important geometric gun parameter. Guns in medium- to high-power tubes are designed, in general, for $\Theta_o \approx 4$ to 12 radians. The approximate range of a_o/r_c, the distance cathode-anode divided by the radius of curvature of the cathode, is 1/3 to 2/3.

The normalized plasma frequency at the anode aperture is $\lambda_a = \omega_{p,a}/\omega$. The practical range for λ_a is 0.01 to about 0.2, which corresponds approximately to microperveances of 0.1 to 1.0 when the final beam size b_o is referred to. Notice that $\omega_{p,o}$, the plasma frequency in the interaction region, is larger than $\omega_{p,a}$ by the factor $m = b_a/b_o$.

In medium- to high-power tubes, $\omega_{q,o}/\omega \approx 0.1$, and the approximate relation holds for $(\omega/u_o)b_o = 1/2$:

$$R_o\lambda_o = \frac{\omega_{q,o}}{\omega} \approx 100 \times P_\mu^{1/2}; \quad \lambda_o = \frac{\omega_{p,o}}{\omega} = m\lambda_a \approx 3.5\times10^2 \times P_\mu^{1/2} \tag{45}$$

The quantity $\sigma_o = kT_c/2eV_o = kT_c/2eV_a$. If T_c is chosen to be 1100 K, which is close to the true cathode temperatures, the anode voltage $V_o = V_a$ may be expressed by σ_o. Since, in tubes designed for about 1-kilowatt power, V_o = 1000 to 10 000 volts, the corresponding σ_o range is 10^{-4} to 0.5×10^{-5}.

The ultimate beam radius is b_o, and the beam radius at the anode aperture is b_a. From equation (28a), $b_a = b(\xi)_{\xi=1} = mb_o$. In modern, high-efficiency tubes, $(\omega/u_o)b_o \approx 0.5$; therefore,

$$b_o \approx 0.5\frac{u_o}{\omega} = 0.5\frac{u_o}{\omega \cdot a_o} \cdot a_o = 0.5\frac{a_o}{\Theta_o} \tag{46}$$

The distance a_o itself may be determined from the relation

$$a_o = \frac{\Theta_o \cdot u_o}{\omega} = 1.29\times10^5 \frac{\Theta_o}{\omega\sqrt{\sigma_o}} \tag{47}$$

where a_o is in meters, Θ_o is in radians, and ω is the angular frequency.

The total area compression ratio A_R is equal to $m^2/[1 - (a_o/r_c)]^2$. In this study, $a_o/r_c = 1/2$ and $2/3$, and $m = 2$ and 3 were used to yield an A_R from 16 to 81. Notice that a given A_R can be achieved by making the compression $1/[1 - (a_o/r_c)]^2$ in the spherical diode larger (smaller) and the subsequent compression m^2 smaller (larger).

Two frequencies, 2 and 10 gigahertz, covering the range of interest to space communications and broadcast satellites, were selected in this study.

Some of the selected beam-gun designs are certainly unrealistic. If, for example, Θ_o is relatively small and the frequency is high, according to equations (46) and (47), both b_o and a_o would be small. Because monotonic beam convergence is required with boundary values specified by equations (28), an unrealistically rapid convergence is required immediately following the anode aperture, that is, at $1.0 \lesssim \xi \lesssim 1.2$. Obviously, a gun designer would not select such an odd combination of parameters; this compilation was made only for the sake of completeness.

The relations (eq. (45)) between the actual tube perveance P_μ, the anodal compression factor m^2, and the relative plasma frequency λ_a^2 are summarized in table I. In deriving the numerical values, $(\omega/u_o)b_o = 1/2$ was assumed.

TABLE I. - RELATIVE PLASMA FREQUENCY AS FUNCTION OF BEAM PERVEANCE AND ANODAL BEAM COMPRESSION

Actual tube perveance, P_μ	Anodal compression factor, m^2	Relative plasma frequency, λ_a^2
0.1×10^{-6}	4, 9	3.1×10^{-3}, 1.36×10^{-3}
1/4	4	$3/4\times10^{-2}$
1/2	4	3/2
1	4	3
1/4	9	1/3
1/2	9	2/3
1	9	4/3

Discussion of Results

The results of this study, plotted in figures 2 to 14, were obtained by solving the expressions for I, U, S, and II on a high-speed, large-storage IBM 7094 computer. Figures 2 to 5 show the quantity S - II plotted against ξ, the normalized distance, between the cathode ($\xi = 0$) and the anode ($\xi = 1$) and at $\xi = 2$, where the compression

is complete for the variable-temperature case. The graphs cover the following range of parameters: $\sigma_o = 10^{-3}$, 10^{-4}, and 10^{-5}; $\lambda_a^2 = 10^{-3}$, 10^{-2}, and 3×10^{-2}; $\Theta_o = 4$ and 8; $a_o/r_c = 1/2$ and $2/3$; $m = 2$ and 3; and $\omega = 2$ and 10 gigahertz. Examination of figures 2 to 5 shows an approximately exponential rise in noise with distance between $\xi = 0$ and $\xi = 1$. Beyond $\xi = 1$, the low-voltage cases ($\sigma_o = 10^{-3}$ and 10^{-4}) exhibit a leveling off of $S - \Pi$, which indicates that S and Π are both approaching their respective asymptotic values at large distances from the cathode. In contrast to this behavior, the high-voltage cases ($\sigma_o = 10^{-5}$) continue to rise steeply with distance beyond $\xi = 1$ for high perveance values ($\lambda_a^2 \geq 10^{-2}$) and less steeply for the low perveance value ($\lambda_a^2 = 10^{-3}$). Notice that, at $\xi = 2$, the values of $S - \Pi$ in high-voltage cases are several orders of magnitude higher than those in low-voltage cases and that, for the same σ_o value, an order of magnitude variation in $S - \Pi$ may be found depending on the size of λ_a^2 and a_o/r_c. The curves show a similar behavior for $0 < \xi < 1$ and branch off for different values of m (e.g., different postanodal compressions). Also, the exponential rise in noise for $0 < \xi < 1$ is in agreement with analytic predictions derived from approximate closed-form solutions in appendix B.

The results of figures 2 to 5 are summarized in figures 6 to 9, where $S - \Pi$ at $\xi = 2$ (which is of interest to tube designers) is plotted against $1/\sigma_o$ (i.e., against a quantity proportional to voltage, with m, λ_a, Θ_o, and a_o/r_c as parameters). An increase in noise with increasing voltage is observed in the range $1/\sigma_o > 10^4$ (i.e., for $V_o > 500$ V), a range of practical importance to designers of tubes with power levels of about 1 kilowatt. (Note that the value $1/\sigma_o = 10^3$ corresponds to a value of V_o of approximately 50 V and is therefore only of academic interest.) The larger the values of λ_a^2 and A_R, the larger is this increase in noise. A significant reduction in noise is possible at $1/\sigma_o = 10^5$, that is, $V_o \approx 5000$ volts and above for $\lambda_o^2 \leq 10^{-3}$. From table I, the latter is seen to correspond to values of $P_\mu < 0.1\times10^{-6}$, which are smaller than conventional values. Another significant conclusion can be drawn from a comparison of figures 7 and 8. The results summarized in both figures were compiled for the same total compression ratio of 36 but for different preanodal and postanodal compressions: in figure 7, the initial compression in the spherical part of the gun is 4 and the final compression is 9; in figure 8, the sequence is reversed. For higher voltages (e.g., $1/\sigma_o > 10^5$), the resulting $(S - \Pi)_{\xi=2}$ is seen to be substantially reduced if the initial compression a_o/r_c is made larger and the subsequent compression smaller. Physically speaking, the "cooling" of beam noise is done more effectively in the low-voltage, large-velocity-spread region than could be achieved if the noise, due to rising temperature, were injected in the high-velocity, negligible-spread region. Thus, guns with perveances $\geq 1/4\times10^{-6}$ should be designed for high initial compression to be more effective in reducing noise.

The preceding discussion is valid, strictly speaking, for fully confined-flow beams. As already mentioned in the INTRODUCTION, less noise should be expected for Brouillon

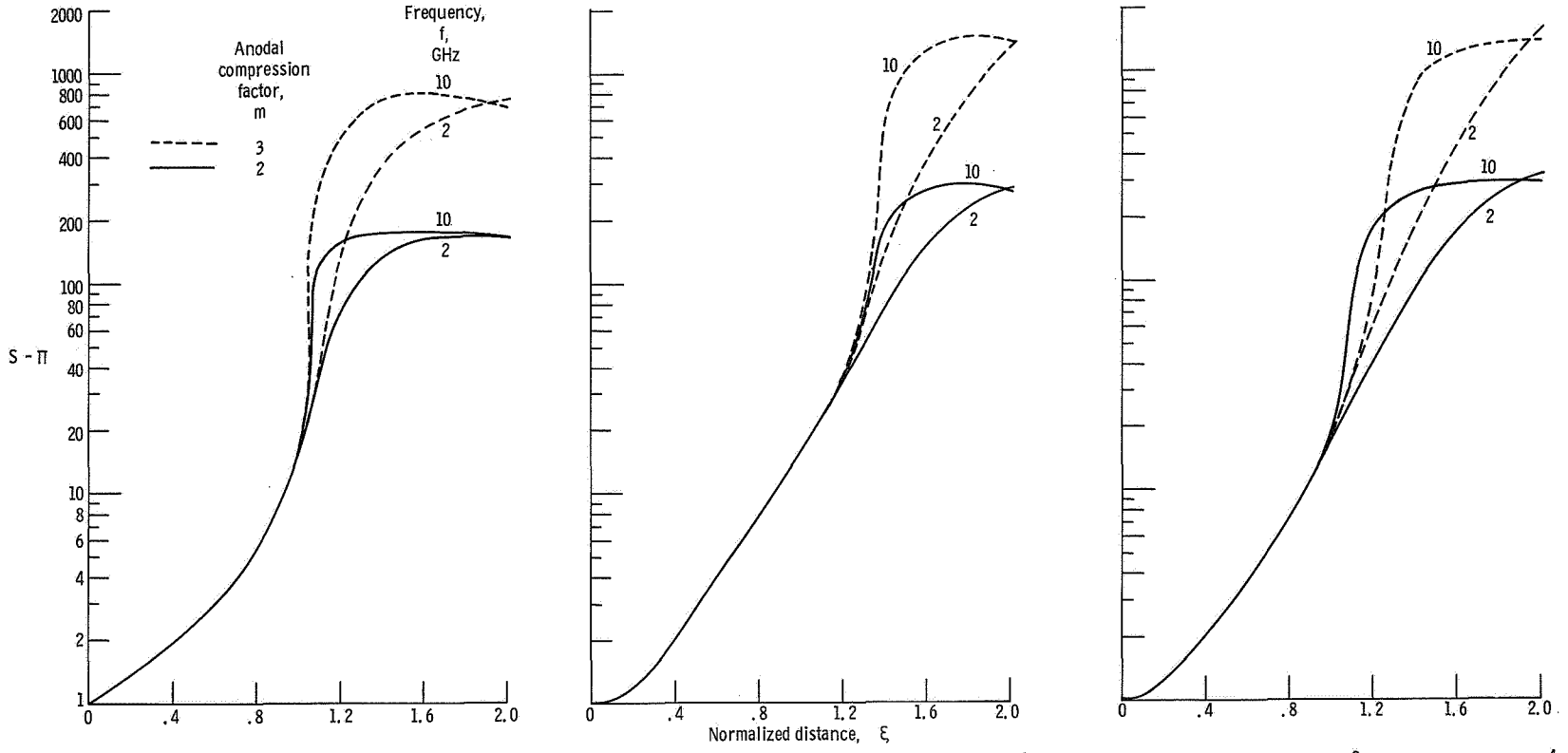

(a) Relative plasma frequency, λ_a^2, 0.03; noisiness, σ, 10^{-3}.

(b) Relative plasma frequency, λ_a^2, 0.01; noisiness, σ, 10^{-4}.

(c) Relative plasma frequency, λ_a^2, 0.03; noisiness, σ, 10^{-4}.

Figure 2. - Quantity S - Π as function of normalized distance for variable-temperature case. Transit time parameter, Θ_0, 8; ratio of cathode-anode distance to cathode radius, a_0/r_c, 1/2.

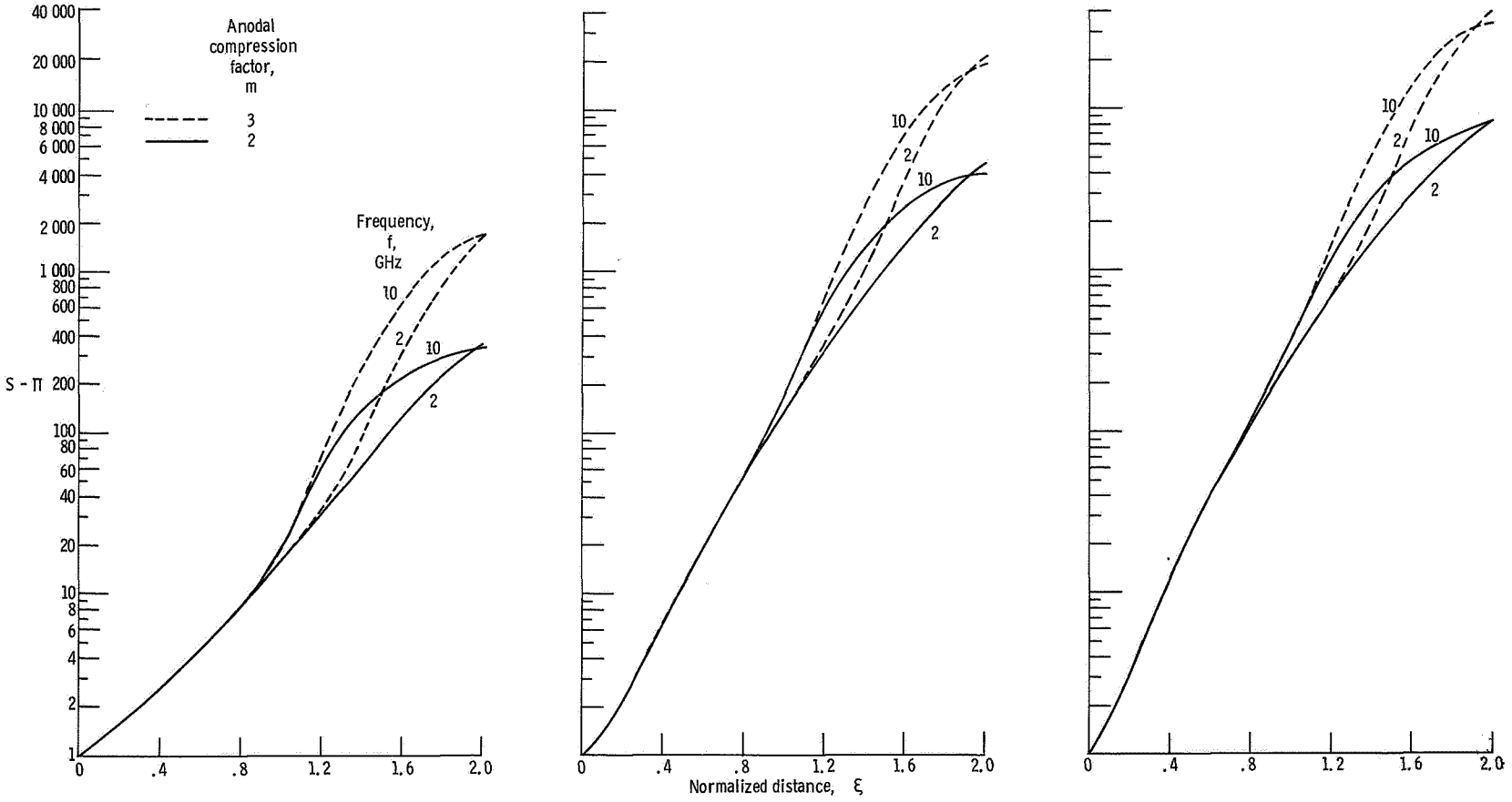

(a) Relative plasma frequency, λ_a^2, 0.001.

(b) Relative plasma frequency, λ_a^2, 0.01.

(c) Relative plasma frequency, λ_a^2, 0.03.

Figure 3. - Quantity S - Π as function of normalized distance for variable-temperature case. Transit time parameter, Θ_0, 8; ratio of cathode-anode distance to cathode radius, a_0/r_c, 1/2; noisiness, σ, 10^{-5}.

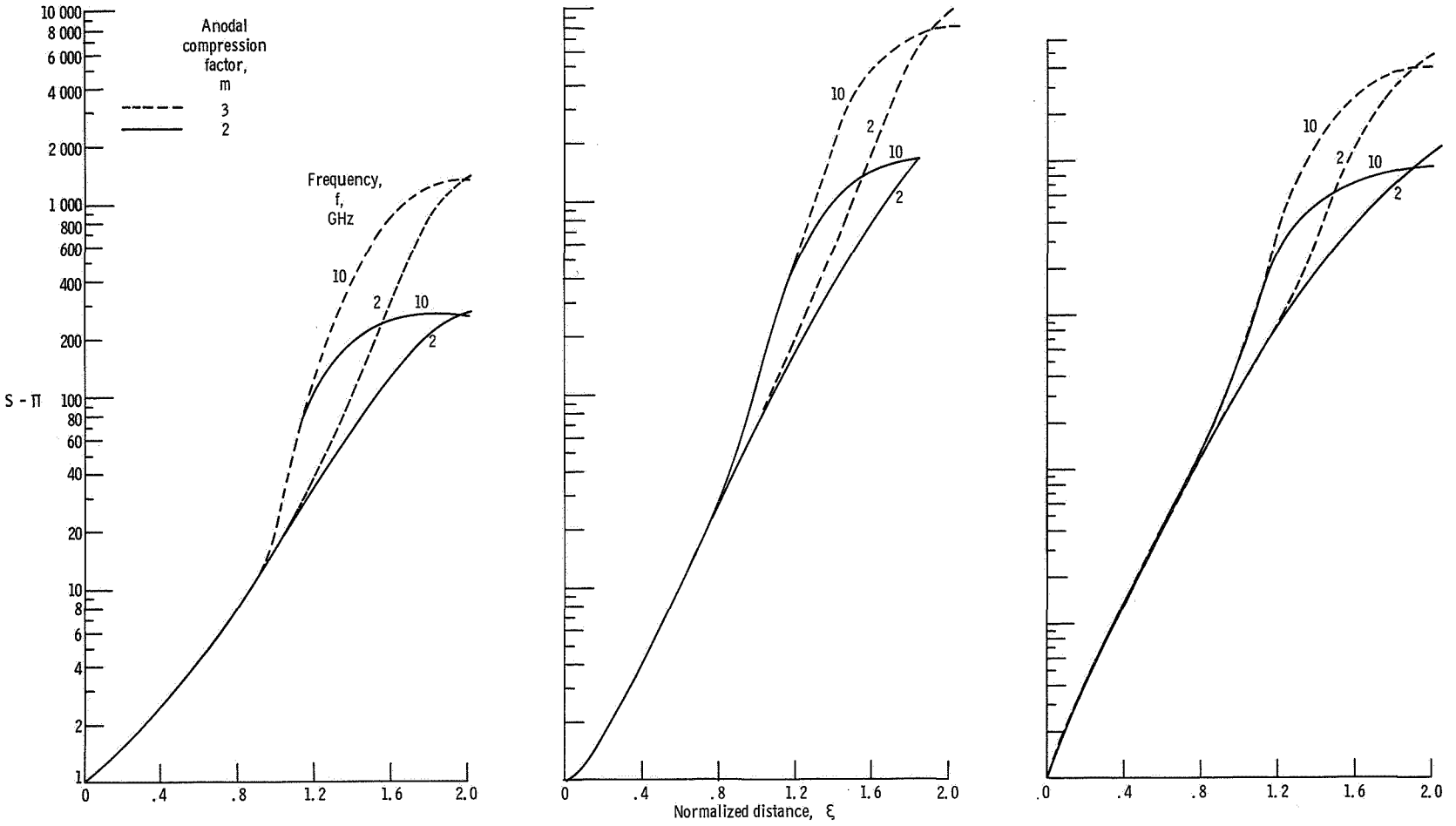

(a) Relative plasma frequency, λ_a^2, 0.001.

(b) Relative plasma frequency, λ_a^2, 0.01.

(c) Relative plasma frequency, λ_a^2, 0.03.

Figure 4. - Quantity S - Π as function of normalized distance for variable-temperature case. Transit time parameter, Θ_0, 4; ratio of cathode-anode distance to cathode radius, a_0/r_c, 1/2; noisiness, σ, 10^{-5}.

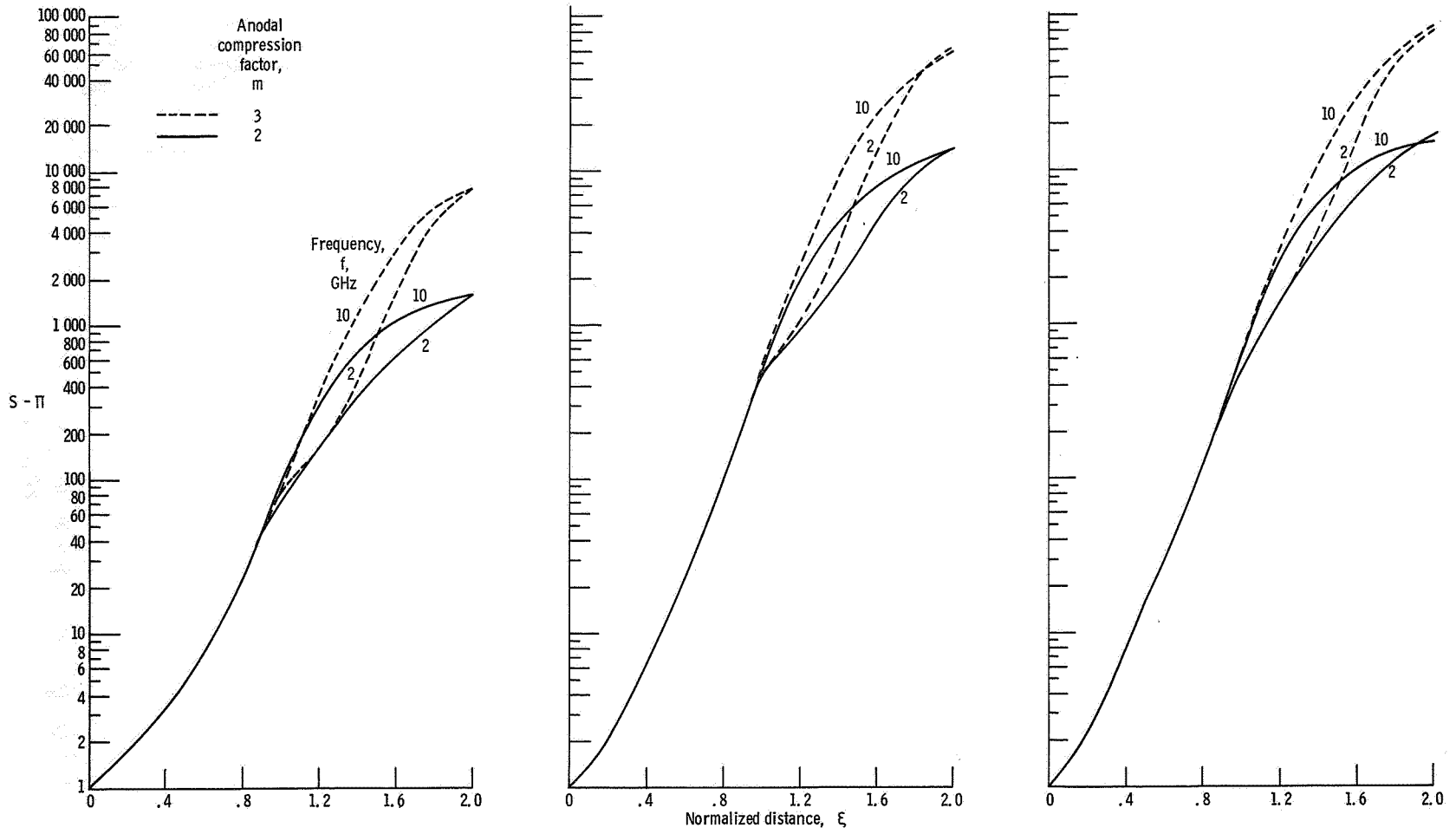

(a) Relative plasma frequency, λ_a^2, 0.001.

(b) Relative plasma frequency, λ_a^2, 0.01.

(c) Relative plasma frequency, λ_a^2, 0.03.

Figure 5. - Quantity S - Π as function of normalized distance for variable-temperature case. Transit time parameter, Θ_0, 8; ratio of cathode-anode distance to cathode radius, a_0/r_c, 2/3; noisiness, σ, 10^{-5}.

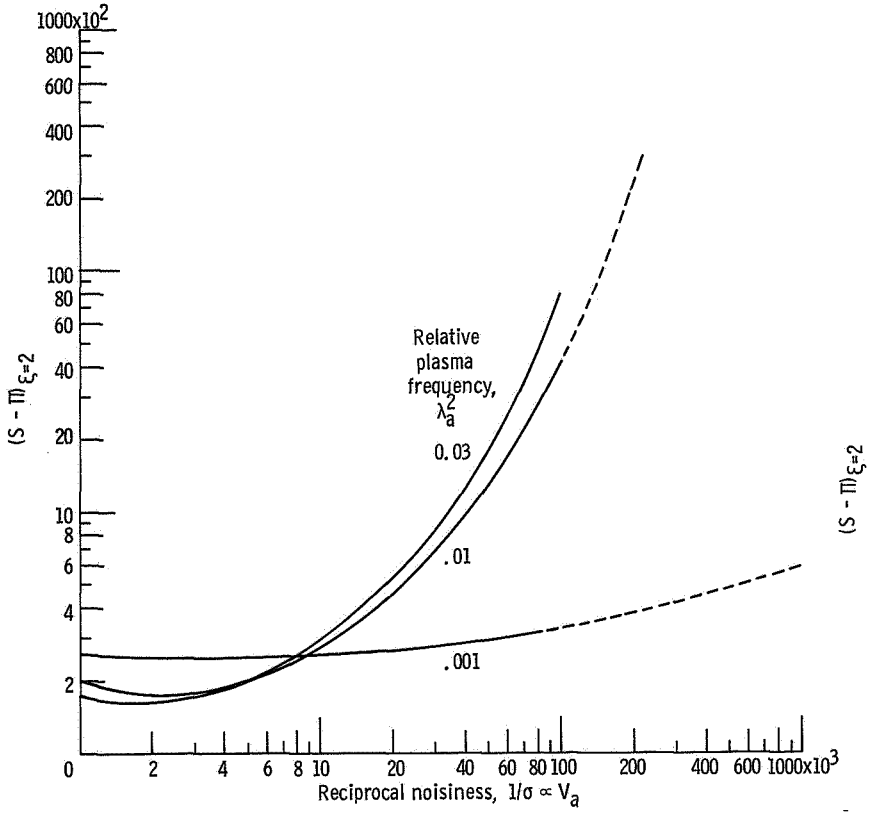

Figure 6. - Quantity S - Π at normalized distance of 2 as function of 1/σ (proportional to voltage) with various values of relative plasma frequency (proportional to perveance) for variable-temperature case. Transit time parameter, Θ_0, 8; ratio of cathode-anode distance to cathode radius, a_0/r_c, 1/2; anodal compression factor, m, 2; area compression ratio, A_R, 16.

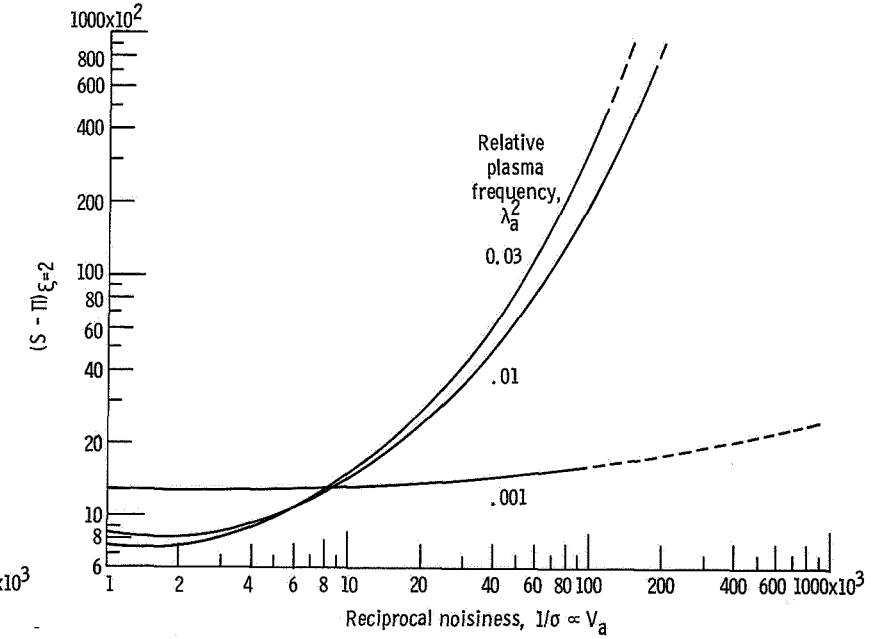

Figure 7. - Quantity S - Π at normalized distance of 2 as function of 1/σ (proportional to voltage) with various values of relative plasma frequency (proportional to perveance) for variable-temperature case. Transit time parameter, Θ_0, 8; ratio of cathode-anode distance to cathode radius, a_0/r_c, 1/2; anodal compression factor, m; 3; area compression ratio, A_R, 36.

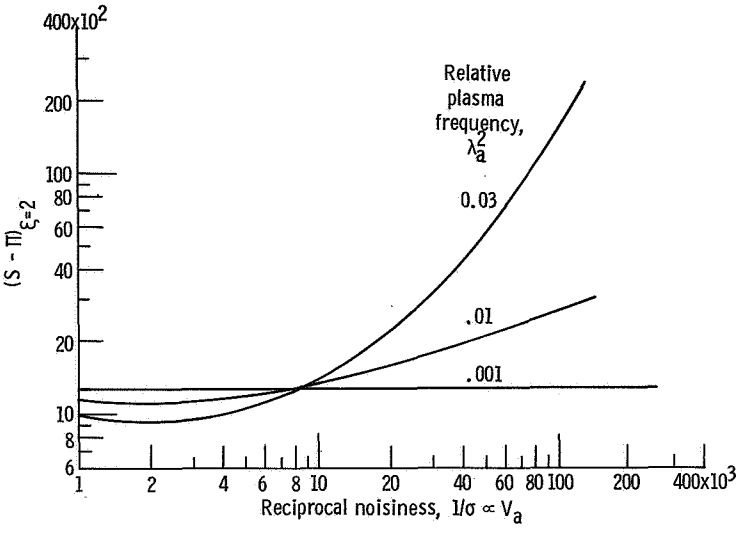

Figure 8. - Quantity S - Π at normalized distance of 2 as function of 1/σ (proportional to voltage) with various values of relative plasma frequency (proportional to perveance) for variable-temperature case. Transit time parameter, Θ_0, 8; ratio of cathode-anode distance to cathode radius, a_0/r_c, 2/3; anodal compression factor, m, 2; area compression ratio, A_R, 36.

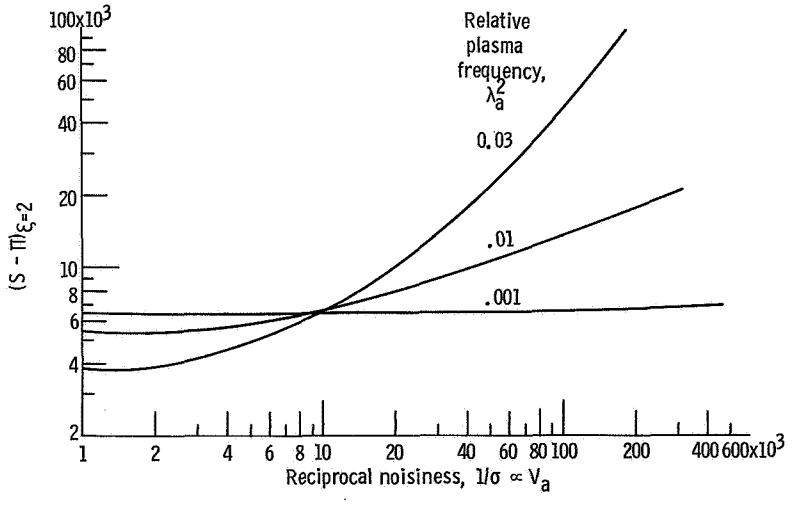

Figure 9. - Quantity S - Π at normalized distance of 2 as function of 1/σ (proportional to voltage) with various values of relative plasma frequency (proportional to perveance) for variable-temperature case. Transit time parameter, Θ_0, 8; ratio of cathode-anode distance to cathode radius, a_0/r_c, 2/3; anodal compression factor, m, 3; area compression ratio, A_R, 81.

focused beams. Although no detailed investigation of this case was made in the present study, it is felt that the difference would not be as large as could be expected for two reasons: First, in the absence of magnetic fields at the cathode surface, some electrons will leave the surface not in normal directions, but rather at all angles between 0^{o} and 90^{o}. This angular spread, which is almost entirely inhibited in confined-flow guns, was not included in the present study, although it certainly contributes to additional noise. Second, an entry into a strong magnetic field always introduces some noise in the high-velocity region where cooling is ineffective.

The discussion now proceeds to figures 10 to 14, compiled for constant-temperature (CT) "ideal" electron beams, ideal meaning the assumption of a flow in which all electrons leave the cathode normal to its surface. Again, this assumption is justified only for confined-flow beams, and therefore in purely electrostatically focused beams (along which constant temperature may be expected only for this ideal situation) will have higher noise in practical cases than that plotted in figures 10 to 14. However, the calculated numbers still represent a useful lower limit of noise. A review of the plots for constant-temperature cases reveals the expected result that the $(S - \Pi)_{\xi=2}$ numbers are two or three orders of magnitude lower than those computed for variable-temperature cases at higher ξ values. At lower ξ values ($\xi < 1/2$), the difference is small because not much noise conversion had taken place yet. Qualitatively speaking, the general parametric behavior is not different from that discussed for variable-temperature cases: figures 10 to 14 show the beneficial effect of higher initial compression (a_o/r_c large) as well as the detrimental effect of higher perveance (λ_a large) on the magnitude of $(S - \Pi)$. Also, a general increase in noise with increasing voltage is clearly evident.

The discussion of the beam-gun parameters is now completed with an examination of the effect of the gun length Θ_o on $(S - \Pi)_{\xi=2}$. A comparison of figure 4 with figures 3 and 5 shows that the effect of Θ_o is not very profound and is only of the order of 20 percent or less. Longer guns ($\Theta_o \geq 8$) seem to be better for high-perveance designs, and

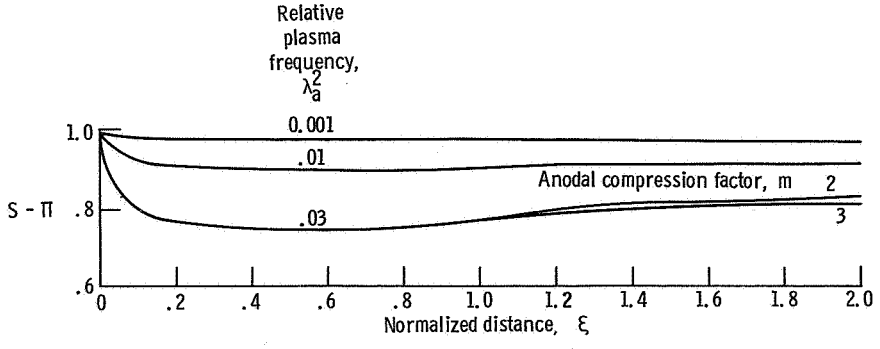

Figure 10. - Quantity S - Π as function of normalized distance for constant-temperature case. Transit time parameter, Θ_o, 8; noisiness, σ, 10^{-3}; ratio of cathode-anode distance to cathode radius, a_o/r_c, 1/2.

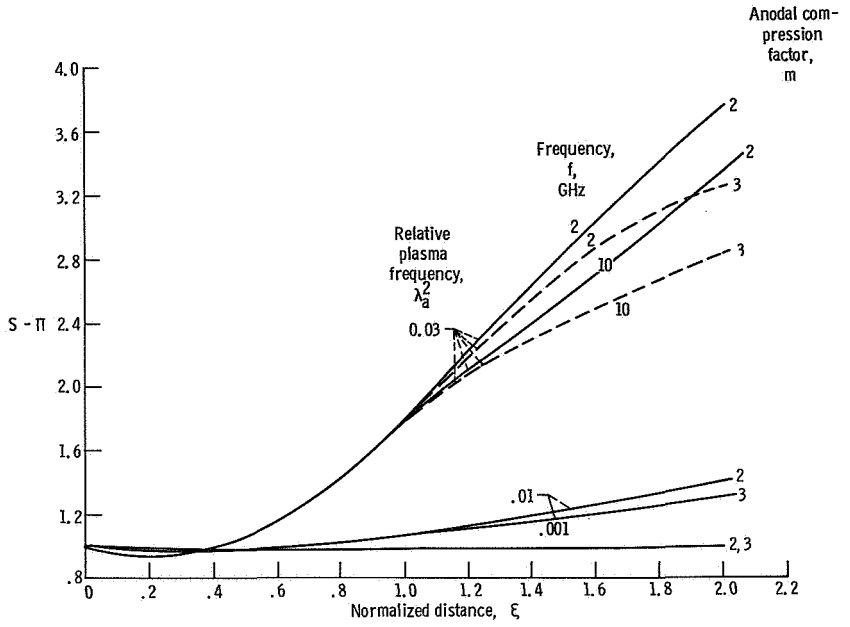

Figure 11. - Quantity S - Π as function of normalized distance for constant-temperature case. Transit time parameter, Θ_0, 4; noisiness, σ, 10^{-4}; ratio of cathode-anode distance to cathode radius, a_0/r_c, 1/2.

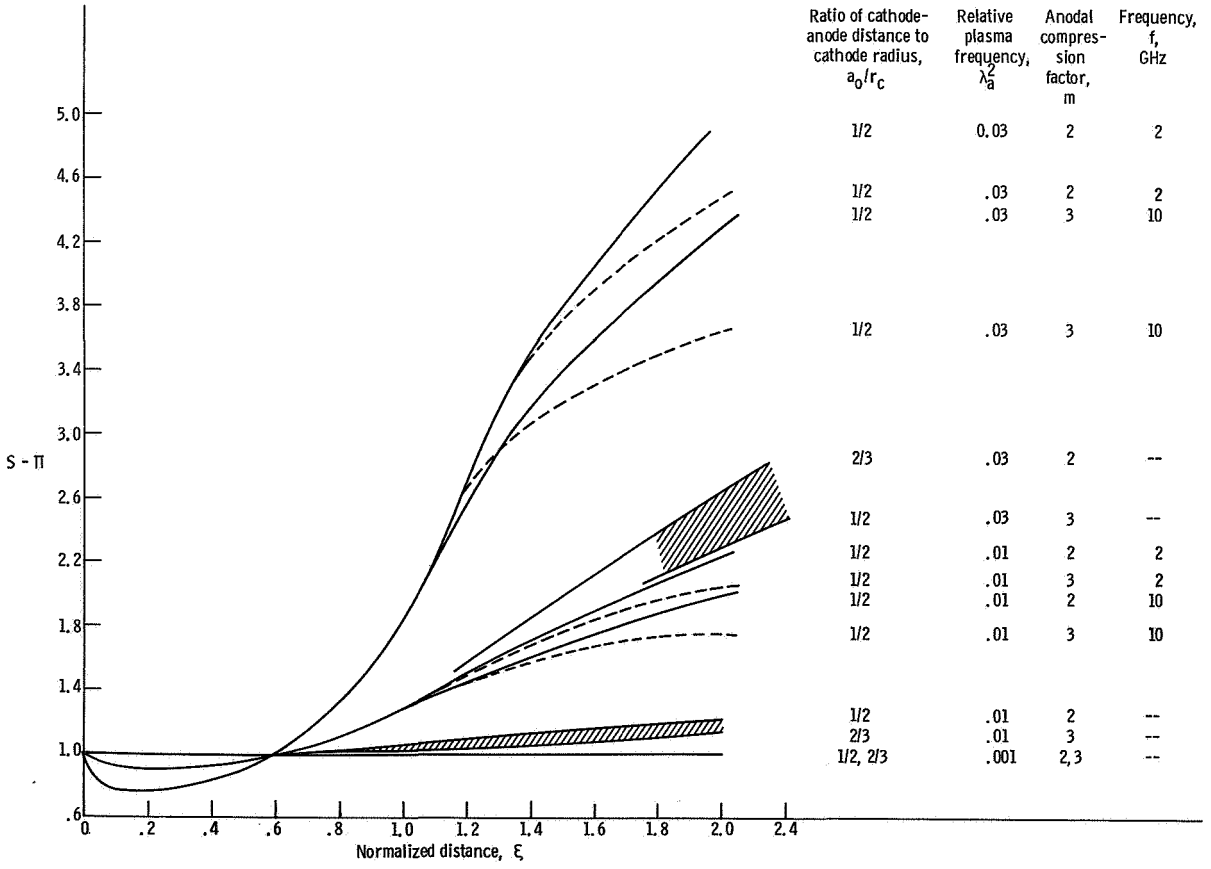

Ratio of cathode-anode distance to cathode radius, a_0/r_c	Relative plasma frequency, λ_a^2	Anodal compression factor, m	Frequency, f, GHz
1/2	0.03	2	2
1/2	.03	2	2
1/2	.03	3	10
1/2	.03	3	10
2/3	.03	2	--
1/2	.03	3	--
1/2	.01	2	2
1/2	.01	3	2
1/2	.01	2	10
1/2	.01	3	10
1/2	.01	2	--
2/3	.01	3	--
1/2, 2/3	.001	2,3	--

Figure 12. - Quantity S - Π as function of normalized distance for constant-temperature case. Transit time paramter, Θ_0, 8; noisiness, σ, 10^{-4}.

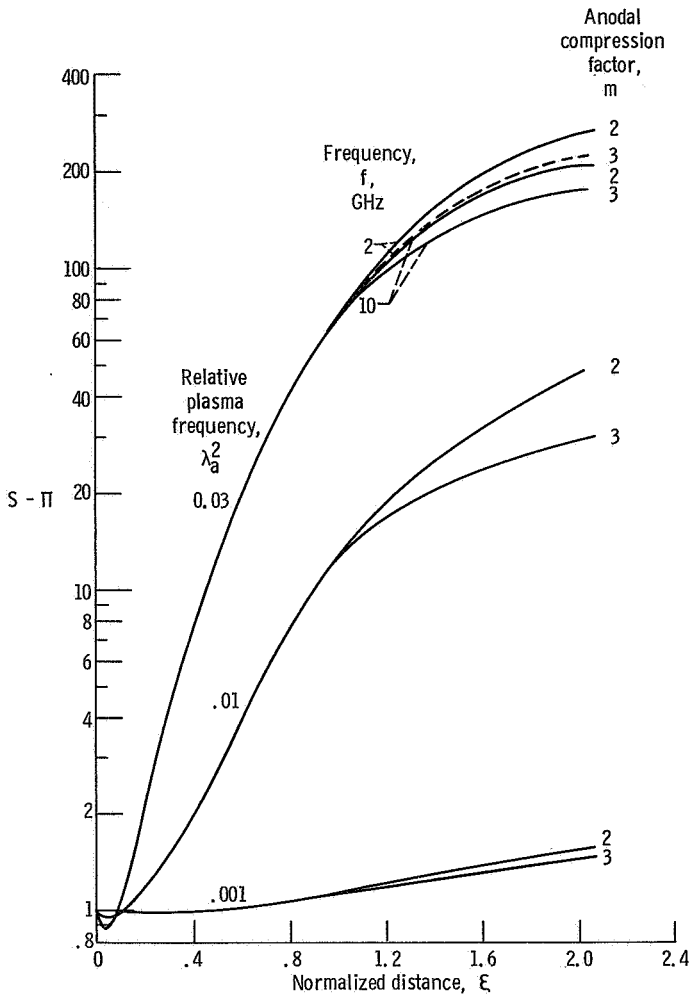

Figure 13. - Quantity S - Π as function of normalized distance for constant-temperature case. Transit time parameter Θ_0, 4; noisiness, σ, 10^{-5}; ratio of cathode-anode distance to cathode radius, a_0/r_c, 1/2.

shorter guns are slightly better for low-perveance designs. A similar behavior may be deduced from constant-temperature cases by comparing figures 12 and 14 (for $\Theta_0 = 8$) with figures 11 and 13 (for $\Theta_0 = 4$). The behavior of either unrealistically short guns ($\Theta_0 < 2$) or very long guns ($\Theta_0 > 12$) was not investigated in detail. However, a few computations made for $\Theta_0 = 2$ and 12 indicated a sharp increase in noise for $\Theta_0 = 2$ compared with cases for $\Theta_0 = 4$ and 8. Additional noise not considered in this study may also be caused by ripple or scallops on the beam (particularly on beams other than confined flow) as a result of improper launching or transition through electric or magnetic lenses.

To conclude the discussion, the error resulting from the omission of the cathode-potential minimum region in the Langmuir-Blodgett equation will be estimated. This omission is equivalent to the assumption 5 (p. 5) which lets the potential minimum coincide with the cathode itself and thus sets the injected noise current equal to the full shot

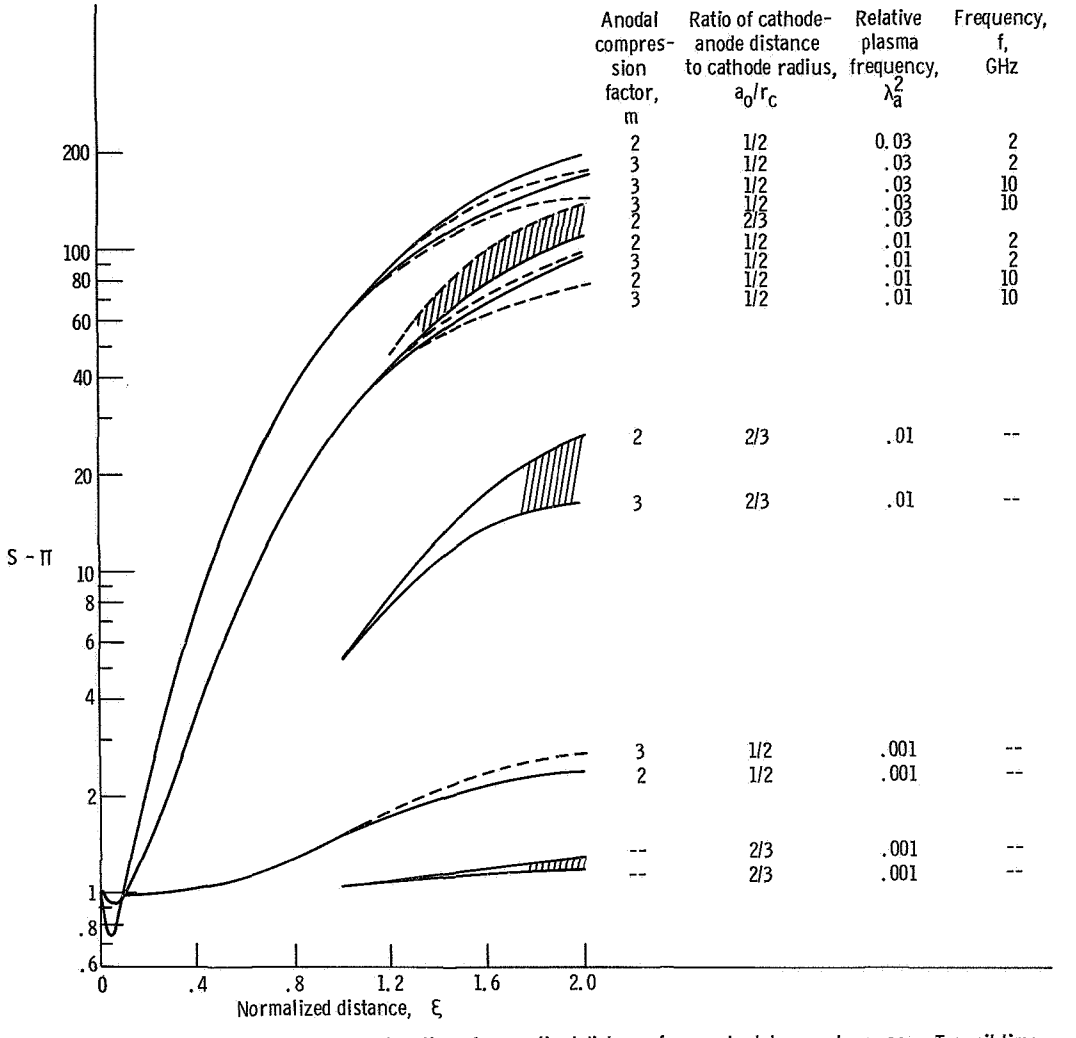

Figure 14. - Quantity S - Π as function of normalized distance for constant-temperature case. Transit time parameter, Θ_0, 8; noisiness, σ, 10^{-5}.

noise. From the exact analysis of the noise behavior in the vicinity of a potential minimum (ref. 12), it is known that the shot noise smoothing factor Γ is approximately 0.3 at radiofrequencies f smaller than the plasma frequency f_{pm} at the potential minimum and approximately 1 at $f > f_{pm}$. Since in high-power microwave tubes, $f_{pm} > 3$ gigahertz, the results of this study may be too high by 5 decibels or less at microwave frequencies below 3 gigahertz and quite accurate above this value. Moreover, it is the range of very high frequencies (e.g., the 10 to 35 gHz range) for which the present study is of special importance because of difficulties associated with generation of power and high-compression ratios. Note, also, that substantial smoothing of noise takes place in the low velocity region following the shot current injection and that the magnitude of the potential minimum being less than 0.5 volt is negligibly small in comparison with the kilovolt anode potential.

SUMMARY OF RESULTS

The following results were obtained from the study of noise propagation along axisymmetric accelerated electron streams for two cases: a longitudinal electron temperature proportional to the beam area compression ratio (confined flow) and a longitudinal electron temperature constant throughout the entire compression region (ideal Brouillon and electrostatic focusing), in both of which flows all electrons leave the cathode normal to its surface:

1. For voltages above a few hundred volts, the noise rises sharply with increasing voltage and less steeply with increasing perveance.

2. For the same total compression ratio, stronger initial compression in the spherical part of the gun followed by smaller subsequent compression produces substantially less noise than the reverse situation, especially at larger perveances, $P_{\mu} \geq 1/4 \times 10^{-6}$.

3. For conventional gun designs, with a transit time parameter $\Theta_0 = 4$ to 10 radians, the noise figure changes only very weakly with Θ_0; however, the noise rises sharply at higher perveances, $P_{\mu} \geq 1/2 \times 10^{-6}$, with decreasing gun length, $\Theta_0 < 2$.

4. The introduction of a new variable, the complex noise convection current divided by the local compression ratio, showed that the basic equations for noise current and electrokinetic voltage become invariant to area transformations, thus reducing the problem to that of one-dimensional Maxwellian streams.

5. The computed noise figures are expected to be fairly accurate for the case of confined-flow streams, the most important being high-power, long-life tubes, and are expected to represent a lower noise limit for Brouillon flow and electrostatically focused beams.

6. For the range of parameters applicable to tubes designed for power levels of approximately a few kilowatts, the computed noise figures ranged between 30 to 60 decibels in variable-temperature cases and between 20 to 30 decibels in constant-temperature cases.

Lewis Research Center,
National Aeronautics and Space Administration,
Cleveland, Ohio, February 5, 1969,
160-21-06-02-22.

APPENDIX A

APPROXIMATE EXPRESSION FOR PLASMA-FREQUENCY-REDUCTION FACTOR

In dealing with electron beams with finite cross sections surrounded by a conducting boundary such as a metallic tube of radius a, the effective plasma frequency is $\omega_q = R \cdot \omega_p$, where R is the well-known reduction factor. For beams having a constant radius b and moving with a constant velocity u_o, $R = R\left[(\omega/u_o)b, (b/a)\right]$ has been computed and plotted for various values of b/a and $(\omega/u_o) \cdot b$ (e.g., see ref. 11). Notice that R approaches 1 for very slow beams, u_o small, or for very high frequencies ω; and $R \to 0$ for the reverse conditions.

The reduction factor R has not yet been computed for beams with a variable velocity u_o and/or a variable radius, b. As shown in figure 1, both beam parameters u and b change simultaneously. However, an approximate solution consistent with the assumption of a homocentric motion with variable cross section may be obtained: Write r for x and assume (see INTRODUCTION) independence of the polar coordinates φ and ϑ for i and E (i.e., $i = i(r)$ and $E = E(r)$, only). The continuity equation is

$$\frac{1}{r^2} \frac{\partial}{\partial r} (r^2 i) = -\frac{\partial \rho}{\partial t} \tag{A1}$$

For the Poisson equation, write (ref. 14)

$$\frac{1}{r^2} \frac{\partial}{\partial r} (r^2 E) = R^2 \frac{\rho}{\epsilon_o} \tag{A2}$$

where $R = R(\omega b/u)$ but not of the coordinate r itself, although both $b = b(r)$ and $u = u(r)$ depend on the position. The formulation equation (A2) is standard for cylindrical beams of constant radius. The integration of the direct-current case, $\partial/\partial t = 0$ in equation (A1), results in

$$i_o(r) = \frac{\text{constant}}{r^2}$$

which is identical with the direct-current continuity equation. Partial differentiation of equation (A2) with respect to t gives

$$\frac{1}{r^2}\frac{\partial}{\partial r}\left(r^2\frac{\partial E}{\partial t}\right)=\frac{R^2}{\epsilon_o}\frac{\partial \rho}{\partial t}=-\frac{R^2}{\epsilon_o}\frac{1}{r^2}\frac{\partial}{\partial r}(r^2 i)$$

or

$$\frac{\partial E(r)}{\partial t}=j\omega E=-\frac{R^2}{\epsilon_o}i(r) \tag{A3}$$

Then, from the earlier notation $r = x$ (eq. (5)),

$$R^2\left[\frac{\omega b(x)}{u(x)}\right]i_1(x)+j\omega\epsilon_o E_1(x)=0$$

Equations (A3) and (5) are believed to be fairly accurate as long as the changes caused by the fluctuations of the radiofrequency field at any instant are larger in effect than those produced by the ordered electron motion. From reference 14, the approximate expression for R is

$$R^2\left(\frac{\omega b}{u},a\right)\approx\frac{1}{1+\frac{3}{4}\left[\frac{1+\frac{b(x)}{a}}{\omega b(x)}\right]^2} \tag{A4}$$

Now, from figure 1, assuming that the shield radius $a \approx r_c$ at $\xi \approx 0$ and $b/a \approx 1/2$ for $\xi \geq 1$ yields

$$b(x)=a\left(1-\frac{x}{r_c}\right)=a\left(1-\frac{a_o}{r_c}\xi\right)$$

$$b(a_o)=a\left(1-\frac{a_o}{r_c}\right) \tag{A5}$$

Note that a, the shield radius, must not be confused with a_o, the distance between cathode and anode (see fig. 1). Substituting equation (A5) into equation (A4) gives (for $0 \leq \xi \leq 1$)

$$R^2_{\xi<1} \approx \frac{1}{1 + \frac{3}{4}\,\frac{\left(2 - \frac{a_o}{r_c}\,\xi\right)^2}{\frac{\omega^2 b^2(x)}{u^2(x)} \cdot \frac{b^2(a_o)}{b^2(a_o)}\,\frac{u^2(a_o)}{u^2(a_o)}}} = \frac{1}{1 + \frac{3}{\beta_a^2 b_a^2}\,\frac{\left(1 - \frac{a_o}{2r_c}\,\xi\right)^2}{\left(1 - \frac{a_o}{r_c}\,\xi\right)^2}\left(1 - \frac{a_o}{r_c}\right)^2 \frac{V(\xi)}{V(a_o)}}$$

$$R^2(\xi)_{\xi<1} \approx \frac{1}{1 + \frac{3\left(1 - \frac{a_o}{r_c}\right)^2}{\beta_a^2 b^2(a_o)}\,\frac{\alpha^{4/3}\left(\frac{a_o}{r_c}\,\xi\right)}{\alpha^{4/3}\left(\frac{a_o}{r_c}\right)}\left[1 + \frac{1}{2}\left(\frac{a_o}{r_c}\,\xi\right) + \frac{1}{2}\left(\frac{a_o}{r_c}\,\xi\right)^2 + \frac{1}{2}\left(\frac{a_o}{r_c}\,\xi\right)^3 + \ldots\right]^2} \qquad \text{(A6)}$$

Notice that $R(0) = 1$ and $0 < R(1) < 1$, and $\beta_a = \omega/u(a_o)$.

The usual design of microwave tubes in the interaction region is such that $\omega b_o/u_o \approx 0.5$. Since the beam radius b_o at the anode aperture is about two to three times b_o, the value in the interaction region, and since $u_a = u_o$ in most cases, $\omega b_a/u_o$ will be approximately 1.5 to 3.0, and R from expression (A6) assumes the value $R(1) \approx 0.7$ for $\xi = 1.0$.

At low values of $\xi \leq 1/4$, where all significant changes in equations for $I(\xi, w_i)$ and $U(\xi, w_i)$ and S, Π, and Λ take place, $V(1/2)$ is $\approx 0.25\ V_a$ and $R(1/4) \approx 0.94$. Thus, R is close to 1 where a more accurate knowledge of it is required.

APPENDIX B

APPROXIMATE SOLUTIONS BY LAPLACE TRANSFORMATION

Longitudinal Temperature Proportional to Beam Compression

Because of the nonintegrability of the transit time functions $\vartheta(\xi, w)$ and their nonlinear characters and the presence of the terms $R^2(\xi)$, $\left[1 - (a_o/r_c)\xi\right]$, and $\left[1 - (a_o/r_c)\xi\right]$ in the kernel, the Volterra integral equation (22) cannot be solved by either one of the two methods most commonly applicable to this type linear integral equations, for example, expansion of the kernel in eigenfunctions, if they exist, or use of the Laplace transformation. The latter method was successfully employed by Bloom and Vural (ref. 4) in solving the noise propagated on a one-dimensional, drifting beam. They approximated their transit time function for low values of σ and Θ_o as a linear function of distance for a drifting beam:

$$\exp\left\{j\Theta_o\left[1 - \left(\frac{1}{1 + 2\sigma w}\right)^{1/2}\right]\right\} \approx \exp(j\sigma w\Theta_o) \tag{B1}$$

In an attempt to gain a qualitative insight into the physics of the phenomena associated with noise propagation on accelerated variable-density beams, an approximate analytical solution will be developed and exact computations made, with the following simplifying assumptions:

(1) The beam is only slightly convergent (e.g., $a_o < r_c$) so that $y < 1$ and $\alpha(y\xi) \approx -y\xi\left[1 + (4/5)y\xi\right]$ according to equation (D3).

(2) The potential profile is only slightly nonlinear.

(3) The measure of the relative velocity spread σ_o is small compared with 1.

Equation (14b) is approximated by

$$\vartheta_s(\xi) = \alpha_a^{2/3}\int_0^{\xi}\frac{d\xi'}{\left[y\xi'\left(1 + \frac{4}{5}y\xi'\right)\right]^{2/3}} \approx \left(\frac{r_e}{a_o}\right)^{2/3}\alpha_a^{2/3}\int_0^{\xi}\frac{d\xi'}{\left(\xi' + \frac{4}{5}y\xi'^2\right)^{2/3}} \tag{B2}$$

Because of assumptions (1) and (2), the integrand in equation (B2) is expanded around a suitable expansion center ξ_o in a Taylor series. Thus,

$$\frac{1}{\left(\xi + \frac{4}{5} y \xi^2\right)^{2/3}} = f_1(\xi_o) + (\xi - \xi_o) f'(\xi_o) + \ldots \tag{B3}$$

with

$$\left.\begin{aligned} f_1(\xi_o) &= \frac{1}{\xi_o^{2/3}\left(1 + \frac{4}{5}\frac{a_o}{r_e}\xi_o\right)^{2/3}} \\ f_1'(\xi_o) &= -\frac{2}{3}\,\frac{1 + \frac{8}{5}\frac{a_o}{r_o}\xi_o}{\xi^{5/3}\left(1 + \frac{4}{5}\frac{a_o}{r_c}\xi_o\right)^{5/3}} \end{aligned}\right\} \tag{B4}$$

Equation (B2) is integrated to the first two terms and yields

$$\vartheta(\xi) = \left(\frac{\alpha_a}{y}\right)^{2/3}\left[f_1(\xi_o)\cdot\xi + f_1'(\xi_o)\left(\frac{\xi^2}{2} - \xi_o\xi + \ldots\right)\right] \tag{B5}$$

Similarly, the integrand of equation (14c) is approximated and expanded into a Taylor series ($y = a_o/r_c$):

$$\left\{\left[y\xi\left(1 + \frac{4}{5}y\xi\right)\right]^{4/3} + \alpha_a^{4/3}\frac{2\sigma_o w}{(1 - y\xi)^2}\right\}^{-1/2} = f_2(\xi_o) + (\xi - \xi_o) f_2'(\xi_o) \tag{B6}$$

$$f_2(\xi_o) = \frac{1 - y\xi_o}{\left\{\left[y\xi_o\left(1 + \frac{4}{5}y\xi_o\right)\right]^{4/3}(1 - y\xi_o)^2 + 2\alpha_a^{4/3}\sigma_o w\right\}^{1/2}} \tag{B7}$$

$$f_2'(\xi_o) = -2y \frac{\sigma_o w \alpha_a^{4/3} + \frac{1}{3}(1 - y\xi_o)^3 (y\xi_o)^{1/3} \left(1 + \frac{4}{5} y\xi_o\right)^{1/3} \left(1 + \frac{8}{5} y\xi_o\right)}{\left\{\left[y\xi_o \left(1 + \frac{4}{5} y\xi_o\right)\right]^{4/3} (1 - y\xi_o)^2 + 2\alpha_a^{4/3} \sigma w\right\}^{3/2}} \tag{B8}$$

The approximated expression for the transit time function is then

$$\vartheta(\xi, w) = \alpha_a^{2/3} \left[f_2(\xi_o) \cdot \xi + f_2'(\xi_o) \left(\frac{\xi^2}{2} - \xi_o \cdot \xi + \ldots\right)\right] \tag{B9}$$

The expressions (B6) and B9) are linearized by setting $\xi^2 = \xi_o \cdot \xi$. Furthermore, for $\sigma_o << 1$, because of assumption (3), the radicands in equations (B7) and (B9) are expanded by taking the first term only. In spite of the fact that $0 < w < \infty$, equation (B9) is a good approximation because of the presence of the weighting factor e^{-w} in equation (22).

With the aforementioned simplifications, the following equations are obtained for the difference of the two transit time functions:

$$\vartheta_s(\xi) - \vartheta(\xi, w) = 2 \frac{\alpha_a^2 \xi}{y^2 \xi_o^2} \sigma_o w \left(1 + \frac{14}{15} y\xi_o - + \ldots\right)$$

$$= \beta_1 \sigma_o w \xi \tag{B10}$$

$$\beta_1 = 2 \frac{\alpha_o^2}{y^2 \xi_o^2} \left(1 + \frac{14}{15} y\xi_o - + \ldots\right) \tag{B11}$$

Similarly, for the difference of $\vartheta_s(\xi) - \vartheta(\xi, w)$, resulting from equation (31a) minus (31b), the following equation is obtained for the range $0 \leq \xi \leq 2$:

$$\sigma_o w \frac{m^2}{\left(1 - \frac{a_o}{r_c}\right)^2} \int_0^{\xi} e^{+\kappa(\xi')\xi'} \, d\xi' \approx \sigma_o w \frac{m^2}{\left(1 - \frac{a_o}{r_c}\right)^2} \int_0^{\xi} e^{\kappa(\xi_o)\xi'} \, d\xi'$$

$$\approx \sigma_o w \frac{m^2}{\left(1 - \frac{a_o}{r_c}\right)^2} \cdot \frac{1}{\kappa(\xi_o)} \left(e^{\kappa(\xi_o)\xi} - 1\right) \approx \beta_2 \xi \qquad \text{(B12)}$$

with the choice of a suitable $1 < \xi_o < 2$.

Now, a new dependent variable is introduced, $J(\xi, w_i) = I(\xi, w_i)$ times the beam compression $(A_R)^{-1}$ defined in equation (34). Thus, from equations (22) and (32),

$$I_1(\xi, w_i) \left(1 - \frac{a_o}{r_e} \xi\right)^2 = J_1(\xi, w_i) \qquad \text{(B13a)}$$

$$I_1(\xi, w_i) \cdot e^{-2 \cdot \xi \cdot \kappa(\xi)} \left(1 - \frac{a_o}{r_o}\right)^2 \frac{1}{m^2} = J_2(\xi, w_i) \qquad \text{(B13b)}$$

Equations (22) and (32) can then be written in the form

$$J_1(\xi, w_i) = e^{j\beta_1 \sigma_o w_i \xi \cdot \Theta_o} + \frac{\lambda_a^2}{j\sigma_o} \left(1 - \frac{a_o}{r_c}\right)^2 \Theta_o R^2(\xi_o) \int_0^{\infty} J_1(\xi', w_i)$$

$$\times \left[1 - \int_0^{\infty} e^{-w} e^{j\Theta_o \beta_1 \sigma(\xi - \xi')w} \, dw\right] d\xi' \qquad \text{(B14a)}$$

$$J_2(\xi, w_i) = e^{j\beta_2\sigma_o w_i \cdot \xi \cdot \Theta_o} + \left(1 - \frac{a_o}{r_c}\right)^2 \Theta_o \frac{\lambda_a^2}{j\sigma_o} \cdot \overline{R^2(\xi_o)} \int_{\xi'=0}^{1} J_1(\xi', w_i)\, d\xi'$$

$$\times \left[1 - \int_0^{\infty} e^{-w + j\Theta_o\beta_1\sigma_o(\xi - \xi')w}\, dw\right] + \Theta_o \overline{R}^2(\xi_o) \int_{\xi'=1}^{\xi} J_2(\xi', w_i)\, d\xi'$$

$$\times \left[1 - \int_0^{\infty} e^{-w + j\Theta_o\beta_2\sigma_o(\xi - \xi')w}\, dw\right] \cdot \frac{m^2\lambda_a^2}{j\sigma_o} \frac{\left(1 - \frac{a_o}{r_o}\right)^2}{m^2} \qquad \text{(B14b)}$$

Notice that $R^2(\xi)$ was approximated under the integral by suitable averages of $\overline{R}^2(\xi_o)$, since $R(\xi)$ is a slowly varying function over ξ. The Volterra integral equations (B14a) and (B14b) for the new function $J_1(\xi, w_i)$ are similar, as already mentioned, to the Volterra equation obtained earlier by Bloom and Vural (ref. 4) for the simple case of a constant-diameter, constant-velocity, and constant-temperature beam. Note that, in the present case, the exponentials are modified by the appearance of $\beta > 1$ and that the relative plasma frequency λ_a^2 is also modified by the factor

$$\left(1 - \frac{a_o}{r_c}\right)^2 \Theta_o \overline{R}^2(\xi_o)$$

Equations (B14a) and (B14b) can be readily solved by the Laplace transformation method, for which is written

$$J(\xi, w_i) = e^{j\beta\sigma_o w_i \xi \cdot \Theta_o} + j\overline{\lambda_a^2} \int_0^{\xi} J(\xi', w_i) \cdot K(\xi - \xi')\, d\xi' \qquad \text{(B15)}$$

$$\overline{\lambda}_a^2 = \left(1 - \frac{a_o}{r_e}\right)^2 \Theta_o^2 \overline{R}_2^2(\xi_o)\lambda_a^2 \qquad \text{(B16)}$$

$$K(\xi - \xi') = +j\Theta_o\beta \frac{\xi - \xi'}{1 - j\beta\sigma_o(\xi - \xi')}$$

$$= \frac{1}{\sigma_o}\left[-1 + \int_0^\infty e^{-w} e^{j\Theta_o\beta\sigma_o(\xi-\xi')w}\, dw\right] \tag{B17}$$

Application of the Laplace transformation and of the convolution integral theorem to $J_1(\xi, w_i)$ yields

$$\left.\begin{aligned} &\int_0^\infty J_1(\xi, w_i)e^{-p\xi}\, d\xi = \mathscr{L}\left[J_1(\xi, w_i)\right] \equiv F(p) \\ &F(p) = \frac{1}{p - j\beta_1\sigma_o\Theta_o w_i} - \bar{\lambda}_a^2 F(p) \cdot \Theta_o\beta_1 \int_0^\infty \frac{\xi e^{-p\xi}}{1 - j\beta_1\sigma_o\xi}\, d\xi \end{aligned}\right\} \tag{B18}$$

$$F(p) = \frac{1}{(p - j\beta_1\sigma_o\Theta_o w_i)\left[1 + j\frac{\lambda_a^2}{\sigma_o^2}\Theta_o\left(\frac{\sigma_o}{p} - j\frac{e^{j(p/\beta_1\Theta_o\sigma_o)}}{\beta_1\Theta_o}\int_{jp/\beta_1\sigma_o\Theta_o}^\infty \frac{e^{-v}}{v}\, dv\right)\right]}$$

Except for the presence of the factors $\beta_1\Theta_o$ and $\bar{\lambda}_a^2$, the algebraic equation (B18) for F(p) is identical with that obtained and discussed earlier by Bloom and Vural for the case of a nonconvergent, drifting beam with constant electron temperature. The quantity F(p) has two purely imaginary poles

$$p = p_i = j\beta_1\sigma_o w_i\Theta_o$$

and

$$p = p_s = -js\beta_1\sigma_o\Theta_o$$

where s is the root of the equation

$$1 - \frac{\lambda^2}{\sigma_o^2}\left(\frac{1}{\beta_1 s} - e^s \int_s^\infty \frac{e^{-v}}{v}\,dv\right) = 0 \tag{B19}$$

The nature of the solutions and their interpretations are described in reference 4; therefore, the results are only summarized herein. The two poles represent the two simple propagating waves with amplitudes A and B, which are given by the residues. In the present case, interest is in medium-power tubes, with p ranging from a few hundred to a few thousand watts, and in conventional perveances $R_\mu \leq 10^{-6}$. Consequently, λ will be approximately 0.1, σ will be between 10^{-4} and 10^{-6}, and $\lambda/\sigma \gg 1$. For the condition $\lambda/\sigma \gg 1$, the amplitude A of the kinematic wave with the propagation constant $p_i = j\beta_1\Theta_o\sigma_o w_i$ dies out to zero, and only the space-charge wave B survives with distance. In addition to the two propagating waves, there is also an aggregate of nonpropagating, Landau-damped waves. The existence of this aggregate may be concluded from the requirement that the vector sum of the amplitudes of all waves at the origin must be 1 so as to represent the unity-injected (normalized radiofrequency) current. Let the aggregate be represented by

$$\left.\begin{aligned} F(\xi) &= \sum_n F_n e^{\sigma_o\Theta_o\xi(jr_n - \alpha_n)} \\ F(0) &= 1 \\ F(\infty) &= 0 \end{aligned}\right\} \tag{B20}$$

Since the discussion in this appendix is concerned with the approximate analytical behavior of the noise problem, a sufficient description is obtained with one nonpropagating fast wave only:

$$F(\xi) \cong F_1 e^{\sigma_o\Theta_o\xi(jr_1 - \alpha_1)} = e^{\sigma_o\Theta_o\xi(jr_1 - \alpha_1)} \tag{B21}$$

The amplitude of the slow propagating wave is

$$B = \mathrm{Res}F(p)_{p=p_s} = \left.\frac{g(p)}{h'(p)}\right|_{p=p_s} \tag{B22a}$$

With

$$g(p)_{p=p_s} = (p_s - j\beta_1\Theta_o\sigma_o w_i)^{-1} = \left[-j\sigma_o\Theta_o\beta_1(s + w_i)\right]^{-1} \tag{B23}$$

and

$$h'(p)_{p=p_s} = \left.\frac{dh(p)}{dp}\right|_{p=p_s}$$

$$h(p) = 1 + j\frac{\lambda_a^2}{\sigma_o^2}\Theta_o\left(\frac{\sigma_o}{p} - j\frac{e^{jp/\beta_1\Theta_o\sigma_o}}{\beta_1\Theta_o}\int_{jp/\beta_1\Theta_o\sigma_o}^{\infty}\frac{e^{-v}}{v}\,dv\right) \tag{B24}$$

one obtains

$$B = \frac{\beta_1 s^2}{(s + w_i)\left(\frac{\lambda_a^2}{\sigma_o^2} - \beta_1 s^2\right)} \tag{B22b}$$

From equation (B19), s is found from integration by parts of $\int_s^{\infty}(e^{-v}/v)\,dv$ to be

$$s \approx \frac{1}{\beta_1}\left(\frac{\bar{\lambda}}{\sigma_o}\sqrt{\beta_1} - \beta_1\right) \tag{B25}$$

The expression for $J_1(\xi, w_i)$ can be written in the form

$$J_1(\xi, w_i) = Be^{-js\beta_1\Theta_o\sigma_o\xi} + (1 - B)e^{\sigma_o\Theta_o(jr_1 - \alpha_1)\xi} \tag{B26}$$

For the desired noise current $I_1(\xi, w_i)$, the following is obtained from equation (B13a):

$$I_1(\xi, w_i) = \frac{B}{\left(1 - \frac{a_o}{r_c}\xi\right)^2}e^{-js\beta_1\Theta_o\sigma_o\xi} + \frac{1 - B}{\left(1 - \frac{a_o}{r_c}\xi\right)^2}e^{\sigma_o\Theta_o(jr_1 - \alpha_1)\xi} \quad \text{for } 0 \le \xi \le 1 \tag{B27a}$$

$$I_1(\xi, w_i) = \frac{m^2}{\left(1 - \frac{a_o}{r_c}\right)^2} e^{-\left[2/(r_c - a_o)\right]} e^{2\kappa(\xi)\cdot\,\xi}\, Be^{-js\beta_2\sigma_o}$$

$$+ (1 - B)e^{\sigma\Theta(jr_1 - \alpha_1)\xi} \qquad \text{for } 1 \le \xi \le 2 \qquad \text{(B27b)}$$

The boundary conditions for $I_1(o, w_i)$ and $\partial I_1(\xi, w_i)/\partial\xi\,\big|_{\xi=0}$ are 1 and $2(a_o/r_c)$ $+ j\beta\Theta_o\sigma_o w_i$, respectively, as may be verified from equation (22). The following equation is obtained from equation (B27a):

$$\left.\begin{aligned} \left[\frac{\partial I_1(\xi, w_i)}{\partial\xi}\right]_{\xi=0} &= 2yB - j\beta\sigma_o\beta_1\Theta_o s + (1 - B)\sigma_o\Theta_o(jr_1 - \alpha_1) \\ &= 2\frac{a_o}{r_o} + j\beta_1\Theta_o\sigma_o w_i \\ r_1 &= \beta_1\frac{Bs + w_i}{1 - B} \\ \alpha_1 &= -\frac{2y}{\sigma_o\Theta_o} \end{aligned}\right\} \qquad \text{(B28)}$$

For $\bar{\lambda}_a/\sigma_o >> 1$, applying equation (B25) to equation (B22b) gives

$$B = \frac{1}{2}\left(1 - \frac{\beta_1 w_i}{s}\right) = \frac{1}{2}\left(1 - \frac{\beta_1 w_i \sigma_o}{\lambda_a\sqrt{\beta_1}}\right) \qquad \text{(B29)}$$

Therefore, $r_1 \approx \beta_1(s + 2w_i)\Theta_o$ and

$$I_1(\xi, w_i) = \frac{B}{(1 - y\xi)^2} e^{-js\beta_1\sigma_o\Theta_o\xi} + \frac{1 - B}{(1 - y\xi)^2} e^{j\sigma_o\Theta_o\beta_1(s+2w_i)\xi} e^{2y\xi} \qquad \text{(B30)}$$

If $s \approx \left(1/\sqrt{\beta_1}\right)\bar{\lambda}_a/\sigma_o$ is taken for $\bar{\lambda}_a/\sigma_o \gg 1$ and substituted into equation (B30), one obtains, for the more important range of $w_i < 10$,

$$I_1(\xi, w_i) \approx \frac{e^{-j\sqrt{\beta_1}\bar{\lambda}_a\Theta_o\xi}}{2(1 - y\xi)^2} + \frac{e^{2y\xi}}{2(1 - y\xi)^2} e^{+j\sqrt{\beta_1}\bar{\lambda}_a\Theta_o\xi}$$

$$= \frac{e^{y\xi}}{(1 - y\xi)^2}\left[\frac{e^{\left(j\sqrt{\beta_1}\bar{\lambda}_a\Theta_o+y\right)\xi} + e^{-\left(j\sqrt{\beta_1}\bar{\lambda}_a\Theta_o+y\right)\xi}}{2}\right]$$

$$= \frac{e^{y\xi}}{(1 - y\xi)^2} \cos\left(\sqrt{\beta_1}\bar{\lambda}_a\Theta_o - jy\right)\xi$$

$$= \frac{e^{y\xi}}{(1 - y\xi)^2}\left[\cos\sqrt{\beta_1}\bar{\lambda}_a\Theta_o\xi \cosh y\xi + j \sin\sqrt{\beta_1}\bar{\lambda}_a\Theta_o\xi \sinh y\xi\right] \qquad \text{(B31)}$$

Equation (B31) is now compared with a corresponding case $I_{1,o}(\xi, w_i)$, obtained from equation (38) for a drifting, nonconvergent, constant-temperature stream ($\beta = 1$, $y = 0$, T_e = constant):

$$I_{1,o}(\xi, w_i) \approx \cos y\xi + j\frac{\sigma}{\lambda} w_i \sin y\xi$$

$$\approx \cos y\xi \qquad \text{for } \frac{\sigma}{\lambda} \ll 1 \qquad \text{(B32)}$$

Thus, a rising electron temperature produces complex current waves whose amplitudes grow even stronger than the beam compression ratio, that is, stronger than the distance squared, and are complex even if the contribution of w_i terms in the exponent and in B of equation (B30) is neglected. The factor $\sqrt{\beta} > 1$ reflects the effect of an accelerated, but nonconvergent, flow. The effective plasma frequency appears larger by a factor $\sqrt{\beta}$ than that in drifting beams. This result may be understood from the nature of the Lagmuir-Blodgett potential shape, which rises slowly over a relatively large distance.

A corresponding similar expression can be obtained for $I_1(\xi, w_i)$ in the range $\xi > 1$ from equation (B27b). Also, by substituting the equations for $I_1(\xi, w_i)$ into the expressions (25) and (33) and by approximating the transit time functions $\vartheta(\xi, w)$ in a manner developed in this appendix, an approximate equation for $U(\xi, w_i)$ could be obtained and,

from the knowledge of I and U, S and Π, could be calculated. However, since U is proportional to powers of $(\lambda/\sigma)^4$, the accuracy of the approximations would no longer be satisfactory. In contrast to $U \gg 1$, the magnitude of $J_1(\xi, w_i)$ is of the order of 1, and the approximate expressions (B30) and (B31) are fairly accurate. In spite of the difficulty of producing a simple and accurate expression for U, the general, qualitative behavior of noise can be predicted to rise with distance much more sharply than constant-temperature beams. This prediction follows from the fact that U increases with I_1, and I_1 grows stronger than the distance squared. Thus, in agreement with experimental findings, much higher noise figures should be expected along magnetically compressed beams.

Longitudinal Temperature Constant

The second case of interest is the converging beam, moving through same potential profile as in equation (B1), but having a constant longitudinal temperature. The analysis of such a case would reveal the effects on the noise behavior of beam convergence and of the direct-current potential alone. The analysis begins with the expansion of the transit time functions $\vartheta_s(\xi)$ and $\vartheta_o(\xi, w)$ (eqs. (14a) and (14c)) in a similar fashion as done in equation (B1). A transit time parameter β_o is obtained:

$$\beta_o = 2\frac{\alpha_a^2}{y^2\xi_o^2}\left[1 - \frac{3}{2}\cdot\frac{4}{5}y\xi_o + \frac{3}{2}\left(\frac{4}{5}y\xi_o\right)^2 \cdots\right] \tag{B33}$$

With the help of equations (B16) and (B17), equation (38) may then be written as

$$I_{1,c}(\xi, w_i) = e^{j\beta_o\Theta_o\sigma_o w_i\xi} + j\bar{\lambda}_a^2 \int_0^\xi \frac{I_{1,c}(\xi', w_i)\cdot K(\xi - \xi')}{(1 - y\xi')^2}\, d\xi' \tag{B34}$$

with $K(\xi - \xi')$ given by equation (B17) and $\beta = \beta_o$. Again, $R^2(\xi')$ has been approximated by a suitable average $\bar{R}^2(\xi_o)$. In its form, equation (B34) cannot be solved by the Laplace transformation method. The solution is achieved by expanding (for $y\xi < 1$)

$$\frac{1}{(1 - y\xi)^2} = 1 + 2y\xi + 3y^2\xi^2 + 4y^3\xi^3 + \cdots \tag{B35}$$

Dropping temporarily the terms containing ξ in equation (B35) makes equation (B33) solvable by Laplace transformation. In analogy to the result obtained in equation (22) for $\bar{\lambda}/\sigma >> 1$ is

$$I_{1,c}(\xi, w_i) = Be^{-js\sigma_o\Theta_o\beta_o\xi} + (1 - B)e^{+j\sigma_o\Theta_o\beta_o(s+2w_i)\xi} \tag{B36}$$

Now the expansion (B35) is introduced under the integral of equation (B34) and the current $I_{1,c}(\xi, w_i)$ modified by the addition of the terms $2y\xi + 3y^2\xi^2 + \ldots$, is called hence-forth, $I_{2,c}(\xi, w_i)$. Thus

$$I_{2,c}(\xi, w_i) = e^{j\beta_o\sigma_o\Theta_o w_i\xi} + j\bar{\lambda}^{-2}\int_0^{\xi} K(\xi - \xi') \cdot I_{2,c}(\xi', w_i)\, d\xi'$$

$$+2yj\bar{\lambda}^{-2}\int_0^{\xi} \xi' \cdot K(\xi - \xi')I_{2,c}(\xi', w_i)\, d\xi' + 3y^2j \cdot \bar{\lambda}^{-3} \ldots \tag{B37}$$

and $K(\xi - \xi')$ is given by equation (B17). Because $y < 1$ and equation (B37) is a linear integral equation, the last terms in equation (B37) may be expected to introduce only a small deviation to the solution (B36) already found, for $I_{i,c}$. One may then assume

$$I_{2,c}(\xi, w_i) \equiv I_1(\xi, w_i) + \Delta I_1(\xi, w_i, y)$$

$$= e^{j\beta_o\sigma_o\Theta_o w_i\xi} + j\bar{\lambda}^{-2}\int_0^{\xi} K(\xi - \xi')\left[I_1(\xi', w_i) + \Delta I_1(\xi', w_i, y)\right] d\xi'$$

$$+ 2yj\bar{\lambda}^{-2}\int_0^{\xi} \xi' K(\xi - \xi')\left[I_1(\xi', w_i) + \Delta I_1(\xi', w_i, y)\right] d\xi' \tag{B38}$$

Subtracting equation (B34) from equation (B38) gives

$$\Delta I_1(\xi, w_i, y) = \bar{\lambda}^{-2}\int_0^{\xi} K(\xi - \xi') \cdot \Delta I_1(\xi', w_i, y)\, d\xi'$$

$$+ 2y\bar{\lambda}^{-2}\int_0^{\xi} \xi' K(\xi - \xi')\left[I_1(\xi', w_i) + \Delta I_1(\xi', w_i, y)\right] d\xi' \tag{B39}$$

In the last term of equation (39), the contribution of ΔI_1 may be neglected under the integral as small compared with I_1 itself. Also, in equation (B39) (which is a correction in itself), a simplified expression may be used for the kernel from equation (B17); that is, for $\sigma_o\Theta_o\beta_o \ll 1$, $K(\xi - \xi') \approx j\Theta_o\beta_o(\xi - \xi')$. After introducing

$$\Lambda_a = -\bar{\lambda}^2\Theta_o^2\beta_o \tag{B40}$$

the following is obtained for equation (B39):

$$\Delta I_1(\xi, w_i, y) = 2y\Lambda_a \int_0^\xi \xi'(\xi - \xi')I_1(\xi', w_i)\, d\xi' + \Lambda_a \int_0^\xi (\xi - \xi')\, \Delta I_1(\xi', w_i, y)\, d\xi' \tag{B41}$$

If the expression (B36) is taken for $I_{1,c}(\xi, w_i)$, is introduced into the first integral of equation (B34), and the first term is called $\varphi(\xi, w_i, y)$, one obtains:

$$\varphi(\xi, w_i, y) = 2\Lambda_a y \int_0^\xi \xi'(\xi - \xi')\Big[Be^{-js\sigma_o\beta_o\Theta_o\xi'} + (1 - B)e^{js\sigma_o\beta_o\Theta_o\xi'} \cdot e^{j'2\sigma_o\Theta_o\beta_o w_i\xi'}\Big]\, d\xi' \tag{B42a}$$

With an error of the order of 1 percent, $B \approx 1/2$ and $e^{j2\sigma_o\beta_o w_i\Theta_o\xi} = 1$ can be substituted for the more important range of $\sigma_o < 10^{-3}$ and $w_i < 10$ and a significant simplification of equation (B42a) can be obtained:

$$\varphi(\xi, w_i) = \frac{2y\Lambda_a\xi}{\bar{\lambda}^2\beta_o\Theta_o^2} \int_0^{\bar{\lambda}\sqrt{\beta_o}\Theta_o\xi} \alpha \cos\alpha\, d\alpha - \frac{2y\Lambda_a}{\bar{\lambda}^3\beta_o^{3/2}\Theta_o^3} \int_0^{\bar{\lambda}\sqrt{\beta}\Theta_o\xi} \alpha^2 \cos\alpha\, d\alpha$$

$$= -2y\xi\left[\frac{2\sin\bar{\lambda}\sqrt{\beta_o}\Theta_o\xi}{\bar{\lambda}\sqrt{\beta_o}\Theta_o\xi} - 1 - \cos\bar{\lambda}\sqrt{\beta_o}\Theta_o\xi\right] \tag{B42b}$$

Note that terms with w_i dropped out of equation (B42b) because of the aforementioned simplifications.

The integral equation (B41) for $\Delta I_1(\xi, w_i, y)$ now assumes the form

$$\Delta I_1(\xi,y) = -2y\xi\left(\frac{2\sin\nu\xi}{\nu\xi} - 1 - \cos\nu\xi\right) + \Lambda_a \int_0^\xi (\xi - \xi')\,\Delta I_1(\xi',y)\,d\xi' \qquad \text{(B41a)}$$

with $\nu = \bar{\lambda}\sqrt{\beta_o\Theta_o}$ for reasons of compactness.

The integral equation (B41a) can be solved with the Laplace transformation method in analogy to the solution of equation (B15), preserving the same analytical approach to the entire problem. Thus,

$$\left.\begin{aligned} F_\nu(p) &= \int_0^\infty e^{-p\xi}\,\Delta I_1(\xi,y)\,d\xi \\ F_\nu(p) &= -\frac{4y}{\nu}\,\frac{\nu}{p^2+\nu^2} + \frac{2y}{p^2} + 2y\,\frac{p^2-\nu^2}{(p^2+\nu^2)^2} + \Lambda_a F_\nu(p)\cdot\frac{1}{p^2} \\ F_\nu(p) &= 2y\nu^2\,\frac{\nu^2-p^2}{(p^2+\nu^2)^3} \end{aligned}\right\} \qquad \text{(B43)}$$

Equation (B43) has two purely imaginary poles of the third order, $p_1 = +j\nu$ and $p_2 = -j\nu$. Their residues are

$$\left.\begin{aligned} \mathrm{Res}F_\nu(p)_{p=+j\nu}e^{p\xi} &= \frac{y}{4}\left[j\left(\nu\xi^2 - \frac{1}{\nu}\right) - \xi\right]e^{j\nu\xi} \\ \mathrm{Res}F_\nu(p)_{p=-j\nu}e^{p\xi} &= \frac{y}{4}\left[-j\left(\nu\xi^2 - \frac{1}{\nu}\right) - \xi\right]e^{-j\nu\xi} \end{aligned}\right\} \qquad \text{(B44)}$$

The Laplace inversion $\mathcal{L}^{-1}\left[F_\nu(p)\right]$ leads to

$$\Delta I(\xi,y) \equiv \mathcal{L}^{-1}\left[F_\nu(p)\right] + \sum_{n=1}^{2} R_{es}F_\nu(p)e^{p_n\xi}$$

$$= \frac{y}{2\nu}\sin\nu\xi - y\,\frac{\nu\xi^2}{2}\sin\nu\xi - \frac{y\xi}{2}\cos\nu\xi \qquad \text{(B45)}$$

The expression for $I_{2,c}(\xi, w_i, y) = I_{1,c}(\xi, w_i) + \Delta I_1$ (eq. (B37)) introduces the effect of convergence, by ΔI_1, on noise propagation in addition to the acceleration effects through a Langmuir-Blodgett potential field. This expression was described earlier in equation (B36) and is now written as

$$I_2(\xi, w_i, y) = Be^{-js\beta_o\sigma_o\Theta_o\xi} + (1 - B)e^{+j\sigma_o\beta_o(s+2w_i)\Theta_o\xi} + \Delta I(\xi, y) \qquad \text{(B46)}$$

Since the imaginary part of equation (B46) is much smaller than its real part, the effect of convergence, by ΔI_1, is to decrease the noise current I_2. For small values of β_o (i.e., for a slightly nonlinear potential profile according to assumption (2) (p. 40) and $\overline{\lambda}\sqrt{\beta_o}\Theta_o\xi < 1$), the approximate expression ΔI is $-(y/3)\nu^2\xi^3$; for small y, $\Delta I \ll 1$. Thus, to a first approximation, this decrease is small. Incidentially, exact computations show that a convergent beam produces less noise current I_2 than its nonconvergent counterpart, provided that both move through the same potential profile and that the nonconvergent beam ends with the same λ_a at the anode aperture. Note, however, that this conclusion is valid only for an electron beam of constant longitudinal temperature, as may be the case with electrostatically focused klystrons.

APPENDIX C

NUMERICAL SOLUTION OF VOLTERRA EQUATIONS

Statement of Problem

Two Volterra-type equations are solved for two unknown, as well as two kernel, functions, all of which are complex functions of two real variables. The constant-temperature case CT and the variable-temperature case VT differ chiefly in their kernels. In both cases, the equations take the forms

$$J(t, w) = f(t, w) - j \int_0^t K_1(t, s)J(s, w)\, ds \qquad \text{for } J(o, w) = 1 \tag{C1}$$

$$U(t, w) = w \cdot f(t, w) - J(t, w) + j \int_0^t K_2(t, s)J(s, w)\, ds \tag{C2}$$

$$f(t, w) = \exp\left\{j\Theta_o\left[\vartheta(t, o) - \vartheta(t, w)\right]\right\} \qquad \text{for } 0 \le t \le 2 \text{ and } w \ge 0 \tag{C3}$$

In the CT case, ϑ is found from

$$\left.\begin{aligned} \vartheta_t(t, w) &= \frac{1}{\sqrt{\dfrac{v(t)}{v(1) + 2\sigma w}}} \qquad 0 \le t \le 1 \\ &= \frac{1}{\sqrt{1 + 2\sigma w}} \qquad 1 < t \le 2 \end{aligned}\right\} \tag{C4}$$

where $\vartheta(o, w) = 0$ (see eq. (35)).

The kernels have the forms

$$K_1(t, s) = L(s)A_R(s)\ 1 - Q_1(t, s) \tag{C5}$$

$$K_2(t, s) = L(s)A_R(s)Q_2(t, s) \tag{C6}$$

where

$$L(s) = \frac{\lambda^2 \Theta_o}{\sigma} (1 - y)^2 R^2(s)$$

and

$$Q_K(t, s) = \int_0^\infty \frac{w^{k-1} \exp(-w) p(t, w)}{f(s, w)} \, dw$$

See equations (30), (38), and (39).

In the VT case, A_R appears in the ϑ equations but not in the kernel equations; that is,

$$\left.\begin{aligned} \vartheta_t(t, w) &= \frac{1}{\sqrt{\dfrac{v(t)}{v(1) + 2\sigma w A_R(t)}}} \qquad 0 \le t \le 1 \\ &= \frac{1}{\sqrt{1 + 2\sigma w A_R(t)}} \qquad 1 < t \le 2 \end{aligned}\right\} \tag{C7}$$

$$K_1(t, s) = L(s)\left[1 - Q_1(t, s)\right] \tag{C8}$$

$$K_2(t, s) = L(s) Q_2(t, s) \tag{C9}$$

See equations (30) to (33).

The problem is, in either case, to solve equations (C1) and (C2) for J and U from t of 1 to 2 for w from 1 to 20. Then, use equations (C10) to (C13) to solve for S(t) - Π(t):

$$\psi(t) = \int_0^\infty |J(t, w)|^2 \exp(-w) \, dw \tag{C10}$$

$$\Phi(t) = \int_0^\infty |U(t, w)|^2 \exp(-w) \, dw \tag{C11}$$

$$\Pi(t) + j\Lambda(t) = \int_0^\infty J(t, w) U^*(t, w) \exp(-w) \, dw \tag{C12}$$

$$S^2(t) = \psi(t)\Phi(t) - \Lambda^2(t) \tag{C13}$$

Each case is either CT or VT. The value of σ is 0.001, 0.0001, or 0.00001; of y or a_o/r_c, 1/2 or 2/3; of Θ_o, 4 or 8; and of λ^2, 0.001, 0.01, or 0.03. The A_R function greater than one uses m - f pairs of (2, 2), (2, 10), (3, 2), and (3, 10).

Method of Solution

Eight steps are involved in the process of solving the problem for a particular set of design values: (1) integrate the function ϑ; (2) compute the Q functions; (3) prepare kernels and ϑ differences for the 0-to-1 part of the problem; (4) integrate J and U from 0 to 1; (5) use these results to compute S(t) - Π(t); (6) compute ϑ, the Q's, the kernels, and the ϑ differences for the 1-to-2 part of the problem; (7) integrate J and U from 1 to 2; (8) use these results to compute S(t) - Π(t). Each step consists of a separate pass on the digital computer. Steps (1) to (3) give card decks of output data; steps (4) to (8) have both input and output data in magnetic tape data files.

Details of Numerical Technique

The program uses two types of integration along curves in the complex plane. Where the chord, is close to the curve, trapezoidal integration is used, and where it is not close, spiral integration is used based on the formulas

$$\int_{t_1}^{t_2} \cos(a + bt)\, dt = (\sin A_2 - \sin A_1)\, \frac{t_2 - t_1}{A_2 - A_1} \tag{C14}$$

$$\int_{t_1}^{t_2} \sin(a + bt)\, dt = -(\cos A_2 - \cos A_1)\, \frac{t_2 - t_1}{A_2 - A_1} \tag{C15}$$

where $A_j = a + bt_j$ and $j = 1, 2$.

The program computes S - Π as 1 - 2Π, even though direct calculation would suffice for many cases of large σ and small λ^2. That this is justified appears from viewing a sample case with small σ (0.00001) and large λ^2 (0.01), where, at t = 2, Π = -13.798, φ = 84 342, ψ = 0.79867, and Λ = -259.17. This leads to $\psi\Phi$ = 67 362, Λ^2 = 67 167, and S^2 = 195. Now this conflicts with the condition S + Π = 1, which is

known to hold everywhere, because if S is 1 - Π or 14.798, its square is 218.98, not 195. However, a slight change in ψ, Φ, and Λ (of less than 0.01 percent) raises $\psi\Phi$ by 12 and lowers Λ^2 by 12, thus giving the correct S. The error in the calculation of these values is greater than this amount; hence, the altered mode of computing S - Π is justified.

The nature of the ϑ equations near zero t for zero w or small w requires special care in the early integration. For this reason, 20 of the 70 values of t from 0 to 1 are below 0.02. The w values need to be finely spaced, near zero because of the nature of the ϑ function and near one because of the exp(-w) weighting of certain integrals. The Q calculations use 101 values of w computed from

$$w(n) = 0.002n^2 \qquad \text{where } n = 0, 1, \ldots, 100$$

The J and U integrations use only 48 of these values (chiefly to lower the time of solution), and they correspond to the following 48 values of n:

0	1	2	3	4	5	6	7	8	9	10	11	12	13	15	17
18	20	21	22	23	24	25	27	28	30	32	33	35	37	38	40
42	43	45	47	48	50	52	53	55	57	58	60	70	80	90	100

Note that these values are finely spaced near a w of 1, or an n of 22 and 23.

APPENDIX D

POWER SERIES FOR LANGMUIR-BLODGETT POTENTIAL

From reference 13, the following relation between V(x) and V(a) may be obtained:

$$V(x) = V(a_o) \frac{\alpha^{4/3}\left(\frac{r}{r_c}\right)}{\alpha^{4/3}\left(\frac{r_o}{r_c}\right)}$$

The α function was calculated by Langmuir and Blodgett in a series

$$\alpha = \gamma - \frac{3}{10}\gamma^2 + \frac{75}{100}\gamma^3 - 0.1432\,\gamma^4 + 0.00216\,\gamma^6 - + \ldots \tag{D1}$$

In the present investigation,

$$\gamma = \ln \frac{r}{r_c} = \ln \frac{r_c - x}{r_c} = \ln \left(1 - \frac{x}{r_c}\right) = \ln \left(1 - \xi \frac{a_o}{r_c}\right) \tag{D2}$$

Since $y = (a_o/r_c) < 1$, γ itself may be expanded into a series and substituted in equation (D1). The result is

$$\alpha\left(\frac{r}{r_c}\right) = \alpha\left(\frac{a_o}{r_c}\,\xi\right) \equiv \alpha(y\xi) = -y\xi\left(1 + \frac{4}{5}y\xi + \frac{17}{24}y^2\xi^2 + 0.662\,y^3\xi^3 + 0.611\,y^4\xi^4 + 0.595\,y^5\xi^5 + 0.57\,y^6\xi^6 + \ldots\right) \tag{D3}$$

In equation (D3), the first three terms are exact; the others are rounded off to the nearest third digit.

APPENDIX E

SYMBOLS

A	area
A_R	total area compression ratio
a	shield radius
a_o	distance between cathode and aperture
b	beam radius
c	$\left[\alpha_a/(a_o/r_o)\right]^{2/3}$ or constants
E	electric field
e	electron charge, 1.6×10^{-19} C
F, f	distribution functions
F_{min}	minimum noise figure
$G(w_i)$	integration constant, eq. (16)
$g(w)$	direct-current distribution function
$H(x, c)$	inhomogeneous part of eq. (11)
$h(p)$	complex function
$I(\xi)$	complex radiofrequency-noise convection current
i	current density
$J(\xi)$	modified complex noise current, $I(\xi)/A_R$
$K(\xi, \xi')$	kernel of integral equation
k	Boltzmann constant, 1.38×10^{-23} J/K
$\mathscr{L}^{-1}\left[F(p)\right]$	inverse Laplace transform, $\equiv f(\xi)$
$\mathscr{L}\left[f(\xi)\right]$	Laplace transform, $\equiv F(p)$
M_e	electron mass, 9.11×10^{-31} kg
m	b_a/b_o
P_μ	beam perveance, $A/V^{3/2}$
p	Laplace variable
$R(x)$	plasma frequency-reduction factor

r	radius
S(w)	unit step function
$S(\xi)$	spectral function of noisiness (normalized), $\left[\psi(\xi)\Phi(\xi) - \Lambda^2(\xi)\right]^{1/2}$
T	temperature, K
t	time
$U(\xi)$	complex electrokinetic noise voltage
u	velocity
V	potential
v	dummy variable
w	energy variable
x	distance
y	a_o/r_c
α	Langmuir-Blodgett function
α_o	$M_e/2kT_c$
α_T	$M_e/2kT_c \times A_R = \alpha_o/A_R$
β	transit time parameter (appendix B)
Γ	cathode opening angle
γ	$\ln r/r_o$ (only in appendix D)
$\delta(w)$	Dirac delta function
ϵ_o	dielectric vacuum constant, 8.854×10^{-12} F/m = C/(J)(m)
η	$e/M_e = 1.759\times10^{11}$ C/kg
Θ_o	transit time parameter, $\omega a_o/(2\eta V_a)^{1/2}$
$\vartheta(\xi, w_i)$	transit time function
$\kappa(\xi)$	beam size polynomial
Λ_a	$-\lambda\Theta_o^2\beta$
$\Lambda(\xi)$	noise power spectral function (imaginary part of)
λ_a	$\omega_{p,a}/\omega$
ν	$+\bar{\lambda}\Theta_o\sqrt{\beta}$
ξ	normalized distance, x/a_o

$\Pi(\xi)$ noise power spectral function (real part of)

ρ space charge density, C/cu m

σ_T $kT_c/2eV_a \times A_R = \sigma_o \times A_R$

$\Phi(\xi)$ $\int_0^\infty |U(\xi, w_i)|^2 e^{-w_i} dw_i$

$\psi(\xi)$ $\int_0^\infty |I(\xi, w_i)|^2 e^{-w_i} dw_i$

ω frequency $\times 2\pi$, Hz

Subscripts:

a anode or aperture

c cathode

e electron

i injection class

l longitudinal

o refers to direct current or ultimate beam size

p plasma parameter

q reduced plasma parameter

s slowest

t transverse

1, 2 radiofrequency quantities, first and second approximations

Superscripts:

— average

$\langle\ \rangle$ average over distribution

REFERENCES

1. Haus, Hermann A.: Noise in One-Dimensional Electron Beams. J. Appl. Phys. vol. 26, no. 5, May 1955, pp. 560-571.

2. Haus, H. A.; and Robinson, F. N. H.: The Minimum Noise Figure of Microwave Beam Amplifiers. Proc. IRE, vol. 43, no. 8, Aug. 1955, pp. 981-991.

3. Watkins, Dean A.: The Effect of Velocity Distribution in a Modulated Electron Stream. J. Appl. Phys, vol. 23, no. 5, May 1952, pp. 568-573.

4. Bloom, Stanley; and Vural, Bayram: Noise on a Drifting Maxwellian Beam. J. Appl. Phys., vol. 34, no. 2, Feb. 1963, pp. 356-363.

5. Siegman, A. E.: Analysis of Multivelocity Electron Beams by the Density-Function Method. J. Appl. Phys., vol. 28, no. 10, Oct. 1957, pp. 1132-1138.

6. Siegman, A. E.; Watkins, D. A.; and Hsieh, Hsung-Cheng: Density-Function Calculations of Noise Propagation on an Accelerated Multivelocity Electron Beam. J. Appl. Phys., vol. 28, no. 10, Oct. 1957, pp. 1138-1148.

7. MacDonald, D. K. C.: Transit-Time Deterioration of Space-Charge Reduction of Shot Effect. Phil. Mag., vol. 40, no. 304, May 1949, pp. 561-568

8. Gandhi, O. P.: Transport of A.C. Disturbances on Electron Beams under Magnetic Compression. International Journal of Electronics. First Series, Vol. 20, 1966, pp. 119-126.

9. Cutler, C. C.; and Hines, M. E.: Thermal Velocity Effects in Electron Guns. Proc. IRE, vol. 43, no. 3, Mar. 1955, pp. 307-315.

10. Danielson, W. E.; Rosenfeld, J. L.; and Saloom, J. A.: A Detailed Analysis of Beam Formation with Electron Guns of the Pierce Type. Bell Syst. Tech. J., vol. 35, no. 2, Mar. 1956, pp. 375-420.

11. Branch, G. M.; and Mihran, T. G.: Plasma Frequency Reduction Factors in Electron Beams. IRE Trans. on Elec. Devices, vol. ED-2, no. 2, Apr. 1955, pp. 3-11.

12. Tien, P. K.; and Moshman, J.: Monte Carlo Calculation of Noise Near the Potential Minimum of a High Frequency Diode. J. Appl. Phys., Vol. 27, 1956, pp. 1067-1078.

13. Langmuir, I.; and Blodgett, Katharine B.: Currents Limited by Space Charge Between Concentric Spheres. Phys. Rev., vol. 24, July 1924, pp. 49-59.

14. Kosmahl, H. G.: Propagation of Space Charge Waves in Diodes and Drift Spaces. IRE trans. on Elec. Devices, vol. ED-6, no. 2, Apr. 1959, pp. 225-231.

NASA-Langley, 1969 —— 10 **E-4316**

NATIONAL AERONAUTICS AND SPACE ADMINISTRATION
WASHINGTON, D. C. 20546

OFFICIAL BUSINESS

FIRST CLASS MAIL

POSTAGE AND FEES PAID
NATIONAL AERONAUTICS AND
SPACE ADMINISTRATION

POSTMASTER: If Undeliverable (Section 158
Postal Manual) Do Not Retu

"The aeronautical and space activities of the United States shall be conducted so as to contribute . . . to the expansion of human knowledge of phenomena in the atmosphere and space. The Administration shall provide for the widest practicable and appropriate dissemination of information concerning its activities and the results thereof."

—NATIONAL AERONAUTICS AND SPACE ACT OF 1958

NASA SCIENTIFIC AND TECHNICAL PUBLICATIONS

TECHNICAL REPORTS: Scientific and technical information considered important, complete, and a lasting contribution to existing knowledge.

TECHNICAL NOTES: Information less broad in scope but nevertheless of importance as a contribution to existing knowledge.

TECHNICAL MEMORANDUMS: Information receiving limited distribution because of preliminary data, security classification, or other reasons.

CONTRACTOR REPORTS: Scientific and technical information generated under a NASA contract or grant and considered an important contribution to existing knowledge.

TECHNICAL TRANSLATIONS: Information published in a foreign language considered to merit NASA distribution in English.

SPECIAL PUBLICATIONS: Information derived from or of value to NASA activities. Publications include conference proceedings, monographs, data compilations, handbooks, sourcebooks, and special bibliographies.

TECHNOLOGY UTILIZATION PUBLICATIONS: Information on technology used by NASA that may be of particular interest in commercial and other non-aerospace applications. Publications include Tech Briefs, Technology Utilization Reports and Notes, and Technology Surveys.

Details on the availability of these publications may be obtained from:

SCIENTIFIC AND TECHNICAL INFORMATION DIVISION

NATIONAL AERONAUTICS AND SPACE ADMINISTRATION

Washington, D.C. 20546